

Abbasi-Malati et al., *BioImpacts.* 2025;15:32624 doi: 10.34172/bi.32624

https://bi.tbzmed.ac.ir/







Autophagy stimulation influenced the angiogenesis and metastasis behavior of human triple-negative breast cancer cells

Zahra Abbasi-Malati¹⁰, Çığır Biray Avci², Parisa Khanicheragh³, Zeinab Aliyari Serej¹, Maryam Sabour Takanlou², Leila Sabour Takanlou², Seyed Ghader Azizi⁴, Reza Rahbarghazi^{5*0}, Zohreh Sanaat⁶, Nafiseh Didar Khosrowshahi⁷, Hassan Amini⁸, Rasoul Hosseinpour^{9,10}

¹Department of Applied Cell Sciences, Faculty of Advanced Medical Sciences, Tabriz University of Medical Sciences, Tabriz, Iran

Article Info



Article Type: Original Article

Article History:

Received: 28 Jul. 2025 Revised: 5 Sep. 2025 Accepted: 21 Sep. 2025 ePublished: 1 Nov. 2025

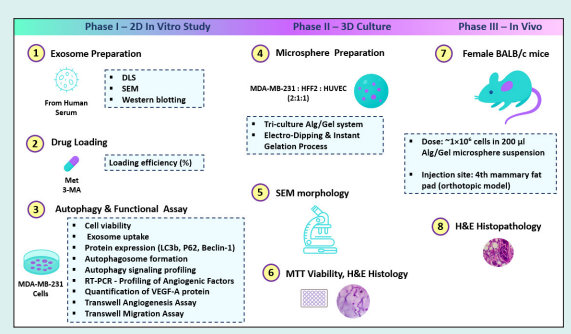
Keywords:

Human breast cancer cells Autophagy Extracellular vesicles Angiogenesis Migration

Abstract

Introduction: Breast cancer (BC) is a devastating condition with high morbidity and mortality rates in females. Autophagy is an early-stage cell response against stressful conditions. Emerging data have revealed the autophagy-angiogenesis interaction in terms of tumor development and metastasis.

Methods: Here, the angiogenesis behavior of human MDA-MB-231 cells was monitored after modulation of autophagy response in the presence of



free 3-methyladenine (3-MA), metformin (Met), or drug-loaded exosomes (3-MA@Exos and Met@Exos). Orthotopic transplantation was done using human BC cell-laden alginate/gelatin (Alg/Gel) microspheres in mice after treatment with Met and/or 3-MA.

Results: Met, and/or Met@Exos increased the cell migration rate and promoted human endothelial cell migration compared to the control cells (P < 0.05). However, these features were blunted in 3-MA and 3-MA@Exos groups (P < 0.05). Flow cytometry analysis revealed that the drug loading into Exos did not influence internalization capacity or cell survival (P > 0.05). ELISA revealed that vascular endothelial growth factor (VEGF) levels were reduced in Met and 3-MA-treated cells, with more pronounced reductions in the free 3-MA groups. Real-time PCR analysis showed diminished expression of several angiogenesis-related genes, except for platelet endothelial cell adhesion molecule-1 (PECAM-1) in the Met@Exos, 3-MA, and 3-MA@Exos groups. Met treatment increased the metastasis and tumor formation in mice mammary glands after orthotopic transplantation of BC tumoroids.

Conclusion: These data indicate that autophagy modulation can alter the angiogenesis and metastatic behavior of human BC cells *in vitro* and *in vivo*. Exos are valid bio-shuttles for the delivery of autophagy modulators in CSC-targeted therapies.

Introduction

Breast cancer (BC) is the most prevalent anaplastic change in females worldwide. Considering the high-rate mortalities and morbidities of BC, attempts have focused on the prevention and development of early-stage

detection methods and therapeutic regimes in the afflicted individuals.² In some cases, the malignant nature of BC cells and inherent resistance to various chemotherapeutics can lead to the failure of medications in the clinical setting.^{3,4} The existence of heterogeneous cell populations



 $*Corresponding \ author: Reza\ Rahbarghazi, Emails: rezarahbardvm@gmail.com; rahbarghazir@tbzmed.ac.ir$

© 2025 The Author(s). This work is published by BioImpacts as an open access article distributed under the terms of the Creative Commons Attribution Non-Commercial License (http://creativecommons.org/licenses/by-nc/4.0/). Non-commercial uses of the work are permitted, provided the original work is properly cited.

²Department of Medical Biology, Faculty of Medicine, Ege University, Izmir, Turkey

³Stem Cell and Regenerative Medicine Institute (SCARM), Tabriz University of Medical Sciences, Tabriz, Iran

⁴Clinical Immunology Research Center, Zahedan University of Medical Sciences, Zahedan, Iran

⁵Stem Cell Research Center, Tabriz University of Medical Sciences, Tabriz, Iran

⁶Hematology and Oncology Research Center, Tabriz University of Medical Sciences, Tabriz, Iran

Stem Cell and Tissue Engineering Research Laboratory, Sahand University of Technology, Tabriz, 51335-1996, Iran

⁸Department of General and Thoracic Surgery, Tabriz University of Medical Sciences, Tabriz, Iran

⁹Student Research Committee, Tabriz University of Medical Sciences, Tabriz, Iran

¹⁰Department of Medical Nanotechnology, Faculty of Advanced Medical Sciences, Tabriz University of Medical Sciences, Tabriz, Iran

within the tumor parenchyma differs in the dynamic growth and metastatic behavior in BC patients. Of note, cancer stem cells (CSCs) with stemness features and resistance mechanisms can trigger the propagation and expansion of cancers to remote sites. CSCs are equipped with several intracellular mechanisms to circumvent immune cell functions and educate other cells in favor of cancer progression and metastasis.⁵⁻⁸ Along with these comments, it is mandatory to develop urgent CSC-based therapies to yield highly efficient therapeutic outcomes in BC patients.⁹

Among different intracellular mechanisms involved in tumor cell resistance against the insulting conditions is autophagy.¹⁰ Autophagy is touted as an earlystage cell response to various pathological and harsh microenvironments to restore the function of the subcellular compartment and eliminate misfolded biomolecules via lysosomal degradation activity.¹¹ The process of autophagy is initiated with the formation of double-membrane autophagosomes by engaging several autophagy-related genes (ATGs), which proceed with the formation of autophagolysosomes, resulting in enzymatic digestion of sequestrated cargo.¹² Despite the stimulatory effects of adaptive autophagy on the dynamic growth of tumor cells against different insults, however, it is believed that excessive autophagic activity can orient the host cells toward injury and death, indicating the double-edged activity of autophagy in biological systems. 13,14 Of course, there is a plethora of studies with conflicting data related to the crucial role of autophagy in tumor cell activities. 15 In the context of cancer biology, the activation of autophagy in CSCs under a hypoxic niche can contribute to the maintenance of stemness features and thus the acquisition of resistance against several chemotherapeutics.¹⁶

CSCs can foster *de novo* blood vessel formation to provide essential elements required for cell proliferation and survival.¹⁷ It has been found that these cells release several pro-angiogenesis factors via the delivery of nanosized extracellular vesicles (EVs), namely exosomes (Exos), or trans-differentiate into endothelial lineage to foster blood perfusion into the deep layer of tumor parenchyma.¹⁸ Emerging data have pointed out the fact that there are shared signaling mechanisms between the angiogenesis and autophagy signaling pathways in the mature endothelial cells (ECs).¹⁹ Whether and how the autophagy response can activate/inhibit the angiogenesis behavior of CSCs is at the center of debate.

In recent years, Exos and other EV types have been used as bioshuttles for the delivery of distinct compounds to the target cells.²⁰ Due to the existence of different internalization mechanisms such as ligand-receptor interaction, direct fusion, micropinocytosis, phagocytosis, and lipid rafts, Exos are easily internalized by normal and cancer cells.²¹ It is thought that Exos can provide a platform to load efficient levels of therapeutics with fewer

side effects, making them appropriate loading platforms for different regenerative purposes.²²

However, the therapeutic effect of autophagy modulation in CSCs using exosome-mediated bioactive substance delivery in angiogenesis and metastasis is unknown. The interest of the study rests on the application of exosomes or natural nanocarriers to load the cells with an autophagy inhibitor (3-MA) or a stimulator (Met) specifically to MDA-MB-231 CSCs in a unique or combined fashion. This approach allows us to dissect the differential effects of autophagy inhibition versus stimulation on tumor progression and angiogenesis. In this regard, we hypothesize that Exo-loaded 3-MA and Met can differentially regulate angiogenic responses and tumorigenic behavior of breast CSCs through modulation of autophagy-related genes and proteins. Accordingly, this study aims to elucidate the angiogenesis behavior of human MDA-MB-231 CSCs after exposure to either free or Exo-loaded agents, thereby providing insights for CSCtargeted therapeutic strategies using EVs.

Materials and Methods Exo isolation from human blood serum

Exos were isolated from human blood samples referred to the clinical laboratory of Shahid Madani Hospital, affiliated with Tabriz University of Medical Sciences. The remnant of serum from healthy individuals was used for the isolation of Exos after the completion of informed consent. Serum samples were collected and transferred to the Cell Culture Lab of the Faculty of Advanced Medical Sciences. Serum samples were centrifuged at 400, 2000, and 10,000 g for 5, 20, and 30 minutes, respectively, to eliminate cells, cell debris, organelles, and particulates. After that, serum samples were pooled to exclude the potential individual effects on the quality and quantity of isolated Exos. Before ultracentrifugation, samples were diluted at a ratio of 1:1 ratio with phosphate-buffered saline (PBS, Sigma-Aldrich, USA). To reduce the confounding impact of viscosity on Exo isolation. Diluted samples were passed through 0.22 µm syringe filters and subjected to ultracentrifugation at 100,000 g for 1 hour (Beckman Coulter Inc. Optima™ TLX-120 ultracentrifuge). After the completion of the ultracentrifugation step, the supernatants were discarded, and exosomal pellets were collected and stored at -80°C for subsequent analyses.²³

Western blotting

Western blotting was utilized to confirm the typical phenotype in isolated Exos by monitoring an Endosomal Sorting Complex Required for Transport (ESCRT) effector, namely TSG101, and tetraspanins such as CD63 and CD81. Exo samples were lysed in ice-cold radioimmunoprecipitation Assay (RIPA) buffers for 30 minutes, followed by centrifugation at 13000g for 20 minutes at 4 °C to yield protein content in the supernatant.

The protein contents were measured using the standard Bicinchoninic Acid Assay (BCA) method (Parstous, Iran). About 10 µg protein was electrophoresed in 10% sodium dodecyl sulfate polyacrylamide gel electrophoresis (SDS-PAGE) gels and transferred onto PVDF membranes. After blocking with 1% bovine serum albumin (BSA; Sigma-Aldrich), membranes were incubated with CD63 (Cat no: sc-5275; Santa Cruz Biotechnology, Inc.), CD81 (Cat no: sc-166029; Santa Cruz Biotechnology, Inc.), and TSG101 (Cat no: sc-7964; Santa Cruz Biotechnology, Inc.) antibodies overnight at 4 °C. The next day, the membranes were washed several times using PBST solution and incubated with HRP-conjugated secondary antibodies at RT for 1 hour. Immunoreactive bands appeared on the X-ray film by using an ECL solution.

SEM imaging

The morphological features of isolated Exos were assessed using an SEM system (Mira-3 FEG SEM microscope, Tescan Co., Czech). For this purpose, 25 µL of diluted Exo samples were placed on the surface of aluminum foil, fixed using 1% paraformaldehyde (PFA) solution for 15 minutes at room temperature, and incubated with an ascending series of EtOH concentrations (30%, 50%, 70%, 90%, and 100%) for 10 minutes at each step. Following dehydration, preparations underwent air drying and sputter-coating with a smooth, thin coat of gold for improved surface conduction. Imaging was done in a vacuum at an accelerating potential of between 10 and 15 kV. This technique provided direct observation of spherical morphology, homogeneity, and smooth Exo surface, thereby consolidating the purity and efficacy of the isolation method.24

Dynamic light scattering (DLS)

The DLS method was employed to measure the hydrodynamic diameter and zeta potential value of isolated human Exos. To this end, diluted Exo samples were analyzed using the DLS system (Model: Anton Paar Litesizer 500, Austria). To achieve this objective, 100 μL of diluted Exosome suspension that was diluted previously in phosphate-buffered saline (PBS) and filtered by a membrane of 0.22 μm was introduced into a quartz cuvette. A scattering angle of 162° was applied at a temperature of 25 \pm 0.1 °C, and each of the samples was assayed thrice for calculating the standard deviation. Average hydrodynamic diameter, polydispersity index (PDI), and zeta potential were noted as parameters of the size distribution and colloidal behavior of Exos, as has been elucidated in earlier literature. 25

Cell culture protocol

In this study, a human BC MDA-MB-231 cell line was purchased from the National Cell Bank of Iran (Pasteur Institute, Tehran) and cultured using high-glucose

content Dulbecco's modified eagle medium (DMEM/HG, Bioidea, Iran) with 10% fetal bovine serum (FBS, Biosera) and 1% Pen-Strep solution (Biosera) under standard conditions (37°C, 95% relative humidity, and 5% CO₂). The exhaust medium was renewed every 3 to 4 days until cells reached 70–80% confluence. Using 0.25% trypsin-EDTA solution (Cat no: B11036; Bioidea), MDA-MB-231 cells were detached and subcultured. All experiments were conducted using cells within passages 3 to 6.

MTT assay

Met treatment

The possible effects of 3-MA and Met were monitored on BC MDA-MB-231 CSC viability after 48 hours using the MTT assay. For this purpose, 1×10^4 MDA-MB-231 cells were plated in each well of 96-well plates (SPL, Korea) and allowed to reach 70-80% confluence. Cells were further grown in basic culture medium supplemented with 1% FBS and 1% Pen-Strep. Once cells achieved confluency, cells were treated for 48 hours in various concentrations of Met (5, 10, 25, 50, 75, and 100 μg/mL; CAS no: 1115-70-4; Sigma-Aldrich). Thereafter, the supernatants were removed and replaced with 200 µL of MTT solution (2 mg/mL; Cat no: M5655; Sigma-Aldrich). The plates were incubated at standard conditions for 4 hours, followed by discarding the MTT solution and the addition of 100 µL of dimethyl sulfoxide (Merck) to dissolve the formazan crystals formed. The optical density of groups was read at 570 nm using a microplate reader (BioTek, USA) and expressed as % of non-treated control MDA-MB-231 cells. In the present study, 10 µM 3-MA (Cat no: M9281; Sigma-Aldrich) was used for the inhibition of autophagy.26 Subsequently, a final dose of 5 µg/mL for free Met was selected for subsequent analyses.

Exo treatment

To monitor possible cytoprotective and/or cytotoxic effects of isolated naïve Exos on human BC CSCs, MDA-MB-231 cells were plated in each well of 96-well plates as mentioned above. Those cells then thrived for 48 hours in a culture medium that was supplemented by 1% Pen-Strep and by 1% Exo-free FBS. In this study, Exos were applied at concentrations of 5, 10, 25, 50, 75, 100, 200, 300, 400, and 500 μ g/mL of exosomal protein. After 48 hours, the viability of Exo-treated groups was determined using MTT. The absorbance was measured at 570 nm, and cell viability (%) was calculated according to the formula: Cell Viability (%) = (OD treated / OD control) × 100. Based on the MTT data, Exos corresponding to 10 μ g/mL of exosomal protein were used for different experimental purposes.

Naïve and drug-loaded Exo uptake

To monitor the internalization rate naïve and modified Exos, naïve and modified Exos, either 3-MA@Exos or Met@Exos, were incubated with $10~\mu g/mL$ Rhodamine B (Sigma-Aldrich) for 30 minutes at room temperature in

the dark. The samples were then resuspended in PBS and ultracentrifuged again ($100,000\times g$, 70 minutes, 4 °C) to exclude unbonded Rhodamine B. Then, Exos were added to the culture medium of pre-cultured MDA-MB-231 cells (corresponding to $10\,\mu g/mL$ of exosomal protein) for 4-6 hours. After that, cells were trypsinized and washed three times with PBS to eliminate non-internalized Exos. The fluorescence intensity was analyzed using BD FACSCalibur and FlowJo software (ver. 7.6) and compared to the control group. All experiments were performed in triplicate, compared to untreated controls.²⁷

Drug loading protocol

Here, in the current experiment, we analyzed the influencing properties of free Met, 3-MA, Met- (Met@ Exos), and 3-MA (3-MA@Exos)-loaded Exos on MDA-MB-231 autophagic response, and angiogenesis capacity after 48 hours. For drug loading, ultrasound waves were utilized to facilitate the loading of Met and 3-MA into the Exolumen. Before drug loading, the maximum absorbance (λmax) values were determined for 3-MA and Met. Serial dilution of Met and 3-MA, including 0.1, 0.2, 0.4, 0.6, 0.8, and 1 mM, was prepared, and the maximum absorbance values were monitored using a UV-Vis spectrophotometer at a wavelength between 200 and 400 nm and recorded as λ max. Exos (~200 µg/mL) were mixed with 200 µg/ mL Met, and/or 72 μM 3-MA in a final volume of 2 ml inside the sterile microtubes. To promote drug loading, samples were maintained inside an ice-cold water bath and exposed to sonication (Bandelin Sonopuls, Germany) at 20% amplitude, six cycles of 30 s ON / 30 s OFF, with a 2-minute cooling interval between cycles. The procedure was continued with the incubation of sonicated samples at 37 °C for 1 hour to recover the exosomal membrane and reduce any abnormal morphologies. After that, the samples were centrifuged at 100,000 g for 70 minutes at 4 °C to yield the Exo pellet. The supernatants were collected, and the absorbance values of non-loaded free Met and/ or 3-MA were measured.^{28,29} The final Exo pellet was resuspended in PBS and stored at either 4 °C (short-term) or -80 °C (long-term) until use. Using GraphPad Prism software (Ver. 8.4.3) and a calibration curve, the absolute concentrations of Met and 3-MA were calculated. Drug loading efficiency was calculated using the following formula as follows Loading efficiency (%) = [(Total drug -Free drug) ÷ Total drug] × 100. Using the MTT assay, the survival rate of MDA-MB-231 cells was again evaluated using MTT after being exposed to Exos, 3-MA@Exos, and Met@Exos for 48 hours using the MTT assay. The steps for the MTT assay were done as above-mentioned.

Autophagy status

Western blotting

MDA-MB-231 CSCs, at an initial density of 5×10^5 cells, were cultured in 6-well plates with DMEM culture

medium supplemented with 10% FBS and 1% penicillin/ streptomycin, and incubated at 37 °C with 5% CO₂, allowed to reach 70-80% confluence. The cells were randomly allocated into six different groups as follows: Control; Exos; 3-MA (10 µM), 3-MA@Exos; Met (5 µg/ mL), and Met@Exos, and maintained for 48 hours. After treatment, total protein was isolated using RIPA buffer. Equal amounts of protein (10 µg per well) were examined by electrophoresis through 12% SDS-PAGE gels and blotting onto PVDF membranes. Membranes were blocked for 2 hours at room temperature in a 5% BSA/TBST solution and incubated overnight at 4 °C with primary antibodies against LC3 (Cat no: 2775, Cell Signaling Technology, USA.), Beclin-1 (Cat no: sc-48341, Santa Cruz Biotechnology, Inc.), and p62 (Cat no: sc-10117, Santa Cruz Biotechnology, Inc.), and several PBST washes, HRP-conjugated secondary antibodies (1:10,000, 1 h, RT) were used for labeling of immunoreactive bands. Using X-ray films and ECL solution, the target proteins were detected in different experimental groups. In this study, β-actin (Cat no: sc-517582, Santa Cruz Biotechnology, Inc.) was used internal control protein. 30,31 Immunofluorescence (IF) staining

Autophagic flux was monitored in MDA-MB-231 cells using IF staining. For this purpose, MDA-MB-231 cells were plated onto each well of an 8-well chamber slide and allowed to reach 70-80% confluence. Cells in different experimental groups were kept under standard conditions for 48 hours, and cells were fixed using 4% paraformaldehyde solution (PFA) for 15 minutes at RT and permeabilized using a 0.1% Triton X-100 solution for 10 minutes. Cells were washed three times with PBS and blocked using 1% BSA for 30 minutes to reduce background staining. Thereafter, cells were incubated with an anti-LC3 antibody (Cat no: ab139484; Abcam) at 4 °C overnight. Cells were again washed three times with PBS and incubated with Alexa Fluor 488-conjugated secondary antibody (Dilution: 1:500, 1 hour). After PBS washes, nuclei were stained using 1 μg/mL DAPI solution (Sigma-Aldrich) for 5 minutes. Slides were mounted and visualized under a fluorescence microscope. The number of cells with LC3 punctata, indicating autophagosomes, was calculated and expressed as LC3+cells/DAPI+LC3+cells.30,31

PCR array analysis

MDA-MB-231 cells were planted in 6-well plates at a seeding density of 5×10^5 cells/well in DMEM/ HG supplemented with 10% FBS and 1% penicillin/ streptomycin solution and maintained in an incubator at 37 °C and 5% CO₂. Once a culture time of 48 h was compatible with the scheduled experimental groups (Control, Exos, 3-MA, 3-MA@Exos, Met, Met@Exos), cells were collected and total RNA contents were isolated using Trizol reagent (Cat no: LB38055; Life Biolab,

Germany) following the manufacturer's instructions. RNA integrity and concentration were evaluated using NanoDrop spectrophotometry. Complementary DNA (cDNA) was synthesized from 0.5 µg RNA using Oligo(dT)₁₅ and Random Hexamer primers and reverse transcriptase (Parstous, Iran). The expression genes belonging to various signal transduction pathways were monitored using the RT² Human Autophagy Profiler array (Cat no: Cat no: PAHS-084Z; Qiagen GeneGlobe) and the Light Cycler 480 Instrument II (Roche). The fold changes were measured using the 2-DACT formula, with GAPDH as internal control. The values of more than 2-fold changes were regarded as statistically significant. This assay was performed using three pooled biological replicates per group. Melting curves were analyzed to confirm the specificity of amplification.

Transwell insert migration of MDA-MB-231 cells

The migration capacity of MDA-MB-231 cells was assessed using a Transwell Insert assay. Briefly, 5×10^4 cells from different groups were resuspended in 200 μL culture medium with 1% FBS and poured onto the Transwell Inserts with 8 µm pore size. The basolateral space was filled with 600-700 µL culture medium containing 10 ng/mL stromal cell-derived factor 1-alpha (SDF-1α; Cat no: 300-28A-50; PeproTech; USA). The chambers were incubated for 48 hours at 37 °C in standard conditions. After that, the inserts were washed with PBS and fixed using a 4% PFA solution, and non-migrated cells on the upper surface of the inserts were cleaned using wet swabs. Migrated cells on the lower surface were submerged in Giemsa stain for 30 minutes. The number of migrated MDA-MB-231 cells at the ventral surface of inserts was counted in at least several serially random high-power fields (HPF).

The paracrine activity of treated MDA-MB-231 cells on EC

To assess whether the secretome of MDA-MB-231 cells can promote/inhibit the migration of ECs, a Transwell Insert assay was conducted. MDA-MB-231 cells were treated with Met, 3-MA, Met@Exos, and 3-MA@Exos for 48 hours. Then, the supernatants were discarded and washed twice with pre-warmed PBS. Cells were again incubated in FBS-free DMEM/HG culture medium for the next 48 hours, and the conditioned media were collected, centrifuged at 400 g, passed through 0.22 µm microfilters, and stored at -80 °C until use. In the next step, 5×104 human umbilical vein endothelial cells (HUVECs; purchased from National Cell Bank of Iran) were resuspended in 200 µL fresh DMEM/HG culture medium and transferred onto Transwell Inserts with $8\,\mu m$ pore size. In the bottom space, 600-700 µL conditioned media from treated MDA-MB-231 cells were added. HUVECs were kept under standard culture conditions for 48 hours. Upon completion of the incubation period,

the cells that migrated to the ventral surface of the inserts were fixed, stained with Giemsa, and counted in several random HPFs.

Monitoring angiogenesis potential using real-time PCR assay and ELISA

The effect of different treatments on the expression of specific factors such as AKT1, IL-8, CDH5, TIMP3, ERBB2, HIF1A, TNF, IFNA1, MMP2, VEGFA, IFNG, NOTCH4, IL-1B, PECAM1, IL-6, and TGFBR1 in MDA-MB-231 cells was evaluated using quantitative real-time PCR (qPCR) (Table 1). In short, after completion of the treatment period, cells were washed using cold PBS, and total RNA contents were isolated utilizing a Trizol (Cat no: LB38055; Life Biolab, Germany) according to the manufacturer's instructions. cDNA synthesis was done using 1 µg of RNA and a reverse cDNA synthesis kit (Parstous, Iran). qPCR reactions were performed in a total volume of 10 μL consisting of 5 μL SYBR Green Master Mix, 0.25 µL forward primer, 0.25 µL reverse primer, 1 μL cDNA, and 3.5 μL deionized water. The reactions were done in the Light Cycler 480 Instrument II (Roche). The relative expression of each gene was calculated using the $2^{-\Delta \Delta CT}$ formula and normalized against the control HPRT1 gene. Along with real-time PCR analysis, protein levels of VEGF in cell lysates were also measured using the Human VEGF-A ELISA kit (Cat no: E-EI-H0111; Elabscience Bionovation Inc.) Cell extracts from treated MDA-MB-231 groups were gathered, centrifuged, and filtered through 0.22 µm filters. 100 µL of each sample or standard was added to pre-coated ELISA wells and incubated at 37 °C for 90 minutes. Three washes later, 100 µL biotinylated detection antibody was added and incubated for 60 min. Then, 100 µL HRP-conjugate was added for 30 minutes, followed by five washes and addition of 90 µL TMB substrate for the development of color. The reaction was halted by the addition of 50 μL stop solution, and the absorbance was measured at 450 nm by a microplate reader. VEGF-A concentrations were estimated from the standard curve, enabling examination of treatment influence on angiogenic potential.

Induction of BC tumoroids Hydrogel preparation

In this study, BC tumoroids were fabricated using Alg/Gel microspheres crosslinked by ionic CaCl_2 solution to recapitulate the 3D tumor microenvironment. For hydrogel preparation, sodium Alg (2% w/v; I-1G, high content of guluronic acid, and MW: 70 kDa; Kimica; Japan) was dissolved in calcium-free CF-KRH solution (pH 7.4) and sterilized with 70% ethanol. Porcine cutaneous Gel (2% w/v; Sigma-Aldrich) was sterilized with chloroform to preserve bio-adhesive properties. CF-KRH solution (pH=7.4) was used as a solvent for the preparation of the solution. Equal volumes of Alg and Gel were mixed

Table 1. Primer sequence

Genes	GenBabk number	Primer sequencing (5'-3')	Product length (bp)
HPRT1	NM_000194.3	F- GACCAGTCAACAGGGGACAT R- GTGTCAATTATATCTTCCACAATCAAG	95
CDH5	NM_001795.5	F- CTTCACCCAGACCAAGTACACA R- TGTTGGCCGTGTTATCGTGA	113
HIF-1α	NM_001530.4	F- AGAGGTTGAGGGACGGAGAT R- GCACCAAGCAGGTCATAGGT	170
PECAM-1	NM_000442.5	F-TGAGTGGTGGGCTCAGATTG R-TGAGTCTAGGTCGGGGAGTG	180
IL-16	NM_000576.3 F- AAACAgATgAAgTgCTCCTTCCAgg R- TGGAgAACACCACTTgTTgCTCCA		391
IL-6	NM_000600.5	F- GGTACATCCTCGACGGCATCT R- GT GCCTCTTTGCTGCTTTCAC	81
IL-8	NM_000584.4	F- AGGGCCAAGAGAATATCCGA R- ACTTGTGGATCCTGGCTAGC	170
NOTCH4	NM_004557.4	F- TGGACGACAACCAGAATGAG R- TCCTCGAACCGGAACTTCT	108
TGFBR1	NM_004612.4	F- GCAGACTTAGGACTGGCAGTAAG R- AGAACTTCAGGGGCCATGT	104
VEGFA	NM_003376.6	F- CTACCTCCACCATGCCAAGT R- GATAGACATCCATGAACTTCACCA	95
TIMP3	NM_000362.5	F- CCTTCTGCAACTCCGACATC R- GCCCCTCCTTTACCAGCTT	66
ERBB2	NM_004448.4	F- CAACTGCACCCACTCCTGT R- GCAGAGATGATGGACGTCAG	87
ММР2	NM_004530.6	F- TAGCTGCTGGCTCACTGTGT R- CTTCAGCACAAACAGGTTGC	88
IFNA1	NM_024013.3	F- AACTCCCCTGATGAATGCGG R- AGTGTAAAGGTGCACATGACG	170

F: forward; R: reverse.

to obtain a final 1% w/v concentration for each polymer. The mixture was stirred overnight at room temperature to ensure homogeneity and remove air bubbles.³³

Fabrication of BC tumoroids using ionic crosslinking

To recapitulate the 3D tumor structure, BC tumoroids were developed by the encapsulation of human umbilical vein endothelial cells (HUVECs), human fibroblasts (HFFF2), and MDA-MB-231 cells at a ratio of 1: 1: 2 inside the Alg/Gel microspheres. Cells were purchased from the National Cell Bank of Iran (Pasteur Institute, Tehran) and expanded in DMEM/HG culture medium with 10% FBS and 1% Pen-Strep. Cells were encapsulated at passages between 3 to 6. About 1×10^6 cells (at the abovementioned ratio) were gently mixed into the hydrogel, maintaining 1% w/v concentration of each polymer. The cell-laden hydrogel was injected into a sterile 21G needle attached to a syringe pump (flow rate of 0.1 mL/minute). The tip of the needle was set 5 cm above a bath of 0.2 M CaCl₂. An electric field of 8 kV was established between the needle (anode) and the bath of CaCl2 (cathode) for droplet generation of uniform shape, and the droplets crosslinked immediately by contacting the Ca2+ ions and resulting in spherical microspheres of diameter 200-300 µm. The microspheres were washed several times with CF-KRH solution to eliminate the non-bound calcium ions. After that, Alg/gel microspheres were cultured in DMEM/HG

culture medium with 10% FBS and 1% Pen-Strep at 37 °C, 5% CO₂ for 48 hours to allow cell attachment, uniform growth, and cell–cell interactions.

Scanning electron microscopy (SEM)

The microstructure and location of cells inside Alg/Gel microspheres were studied using SEM. The Alg/Gel microspheres were fixed inside a 4% paraformaldehyde solution for 20 minutes and lyophilized. After gold sputtering, the morphology and structure of microspheres were studied using an SEM apparatus.

Effect of 3-MA and Met on BC tumoroid viability

To assess the cytoprotective and/or cytotoxic effects of Met (5 μ g/mL; based on preliminary 2D MTT data) and 3-MA (1.5 μ g/mL; according to previous studies confirming autophagy inhibition via PI3K/AKT/mTOR signaling) on BC tumoroid cells, microspheres were allocated into three groups: Control, 3-MA, and Met groups. Cells were treated for 48 hours under standard conditions (37 °C, 5% CO₂). After that, the supernatant was discarded, and microspheres were washed with PBS and incubated with 2 mg/mL MTT solution for 3-4 hours at 37 °C. After removing the solution, DMSO (100 μ L/well) was added to solubilize the formazan. The optical density was read at 570 nm using a microplate reader, and the survival rate was reported as % of the control group.

Monitoring the cell density inside BC tumoroids

The density and location of tumoroid cells inside the Alg/ Gel microspheres were studied using hematoxylin-Eosin (H & E) staining. After treatment of BC tumoroids with 3-MA and/or Met, Alg/Gel microspheres were fixed in 4% PFA, and 5 µm-thick slides were prepared from paraffinembedded blocks. The density and distribution of BC tumoroids were counted and reported per microsphere. Orthotopic injections of BC tumoroids into the mouse

mammary gland

The possible effect of autophagy stimulation/inhibition on BC tumoroid dynamic growth in in vivo conditions, an orthotopic injection of cell-laden Alg/Gel microspheres was done in the mouse mammary glands. BC tumoroids (MDA-MB-231, HUVEC, HFF2) inside the Alg/Gel microspheres were pretreated with drugs for 48 hours. The treatment groups included: induction of autophagy: Met at 5 µg/mL and inhibition of autophagy: 3-MA at 1.5 μg/mL. Microspheres were retrieved at 48 hours, centrifuged, washed off remaining medium and free drug, and prepared for injection.

Eighteen mature female Balb/c mice weighing 22-25 g were accommodated in the animal house of the Faculty of Advanced Medical Sciences, Tabriz University of Medical Sciences, with 12 h light/12 h darkness, standard temperature, and relative humidity for 7 days. Animals were allowed access to chewing pellets and tap water ad *libitum*. All phase of the study was approved by the ethics

committee of the Vice President of Scientific Technology and Knowledge Council for Development of Regenerative Medicine and Stem Cells Technologies, and the Research Ethics Committee of Tabriz University of Medical Sciences (Ethical code: IR.TBZMED.VCR.REC.1401.392). Mice were anesthetized using a combination of Xylazine (10 mg/mL) and Ketamine (80 mg/mL). About 200 μL of solution containing Alg/Gel microspheres with a total number of $\sim 1 \times 10^6$ cells was injected into the fourth mammary fat pad (orthotopic site) to mimic a physiological breast tumor microenvironment. Mice were also immunocompromised using 200 mg/mL cyclophosphamide (Endoxyna^{*}) to prevent the rejection of xenogeneic cells. After two weeks post-injection, mice were euthanized using an overdose of ketamine and xylazine. The transplanted mammary tissue and surrounding tissue were retrieved and fixed for 24 hours in 10% neutral buffered formalin to preserve cellular and tissue structures. Specimens were dehydrated by increasing alcohol series, cleared in xylene, and paraffinembedded. 5 µm-thick sections were loaded and mounted onto glass slides. Histological changes such as cellular structure, nucleus and cytoplasm features, inflammation, necrosis, cell migration, and microsphere integrity were noted by performing H&E staining.

Statistical analysis

Data (Mean ± SD) were analyzed using One-way ANOVA with Tukey post hoc and GraphPad Prism software

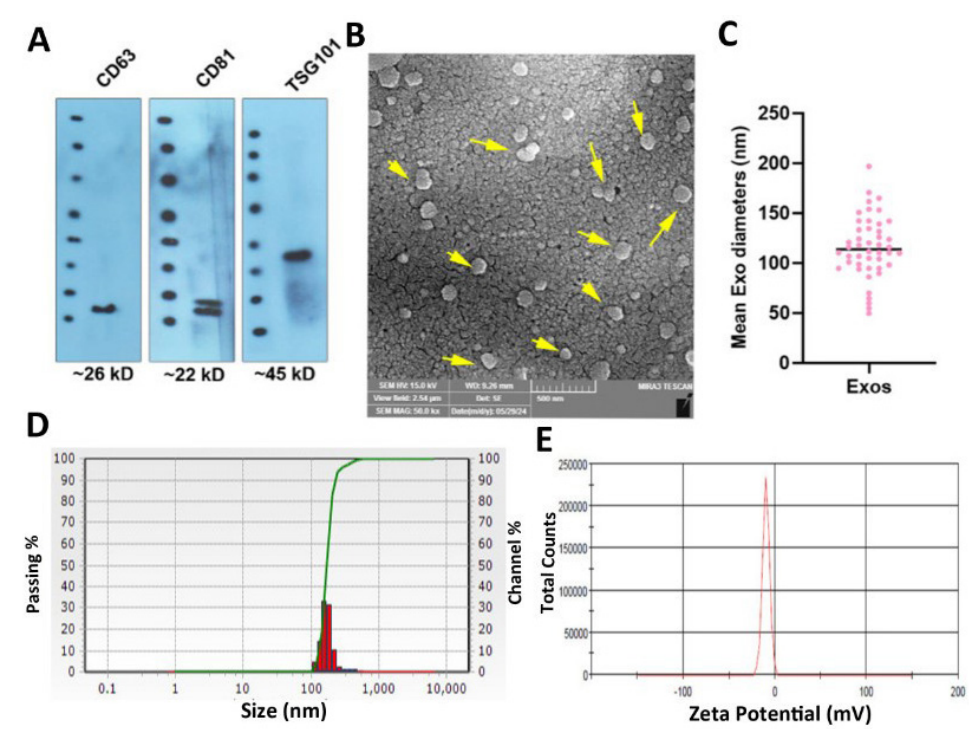


Fig. 1. Physicochemical properties of isolated Exos from human blood samples. Western blotting revealed the existence of identical markers such as CD63, CD81, and TSG101 in enriched Exos (A: data were obtained from three pooled samples). The blots were cropped and presented in panel A, SEM images show the typical spherical morphologies with an average size of 116±84 nm (B and C; n=3). DLS analysis of enriched Exos revealed a hydrodynamic diameter of 202 ± 52.59 nm and a zeta potential value of -12.76 ± 4.57 mV (n = 3).

(version 8.4.3). Assays were done in three technical and statistical replicates, otherwise mentioned. P values < 0.05 were considered statistically significant.

Results

Exos purification and immunophenotyping

The entity of isolated Exos was confirmed using different analyses (Fig. 1A-E). Western blotting indicated the existence of tetraspanins (CD63, CD81), and ESCRT system effector (TSG101) in the enriched Exos in human blood samples (Fig. 1A). Full-length blots are provided in Fig. S1 for transparency (Supplementary file 1). SEM images confirmed nano-sized spherical particles with an average diameter of 116±84 nm (Fig. 1B-C; yellow arrows). Using DLS, it was shown that the mean hydrodynamic diameter of Exos reached 202±52.59 nm while the zeta potential value of -12.76±4.57 mV was achieved, indicating appropriate physicochemical properties of isolated Exos from the human blood (Fig. 1D-E).

Survival assay

In the present study, human MDA-MB-231 cells were exposed to various concentrations of Met, ranging from 5 to $100~\mu g/mL$ for 48 hours (Fig. 2A). Data revealed the statistically non-significant difference in the viability of cells after treatment with different doses of Met when compared to the non-treated control group (Fig. 2A).

Likewise, treatment of MDA-MB-231 cells with Exos corresponding to various exosomal protein contents yielded non-significant differences (Fig. 2A; P > 0.05). In the groups that received Exos equal to exosomal proteins ranging from 5 to 50 µg/mL, relatively similar survival rates were obtained. Although the increase in Exo doses from 75 to 500 µg/mL slightly increased the survival rate, these data did not reach statistically significant differences.

Drug loading

UV-Vis spectroscopy analysis revealed a maximum absorption wavelength (λ_{max}) for Met at 233.5 nm (Fig. 2B). Thus, the absorption rate was used to calculate the drug loading percentage in conjunction with the formula specified in the methods section. Based on the data, the loading efficiency of Met on Exos was 23%. Notably, the λ_{max} for 3-MA was identified at 272 nm, with a loading efficiency of 64% onto Exos. These percentages reflect the levels of drugs, either Met or 3-MA, incorporated into the exosomal lumen.

Loading protocol did not affect the BC cell survival rate and Exo internalization

MTT data revealed the lack of statistically significant differences in terms of viability in Exos, 3-MA@Exos, and Met@Exos as compared to the non-treated control cells after 48 hours (Fig. 3A). These data indicate that the drugloaded Exos and naïve Exos did not exert any tumoricidal

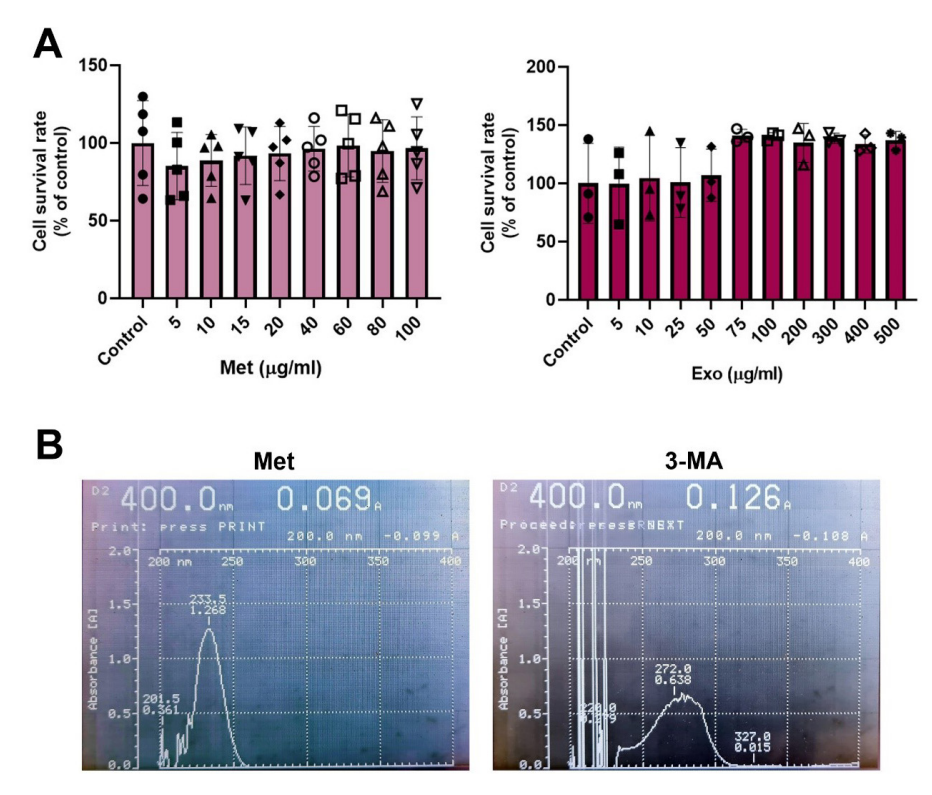


Fig. 2. MTT assay. The survival rate of MDA-MB-231 cells in response to different doses of Met after 48 hours (A). Data revealed non-significant differences in terms of cell viability in different groups as compared to the control cells (n=4; P>0.05). Measuring the viability of MDA-MB-231 cells after treatment with Exos equals exosomal proteins, for 48 hours. Statistically non-significant differences were obtained in comparison with the control group (n=3; P>0.05). Absorption spectra of Met and 3-MA using UV-Vis assay (B).

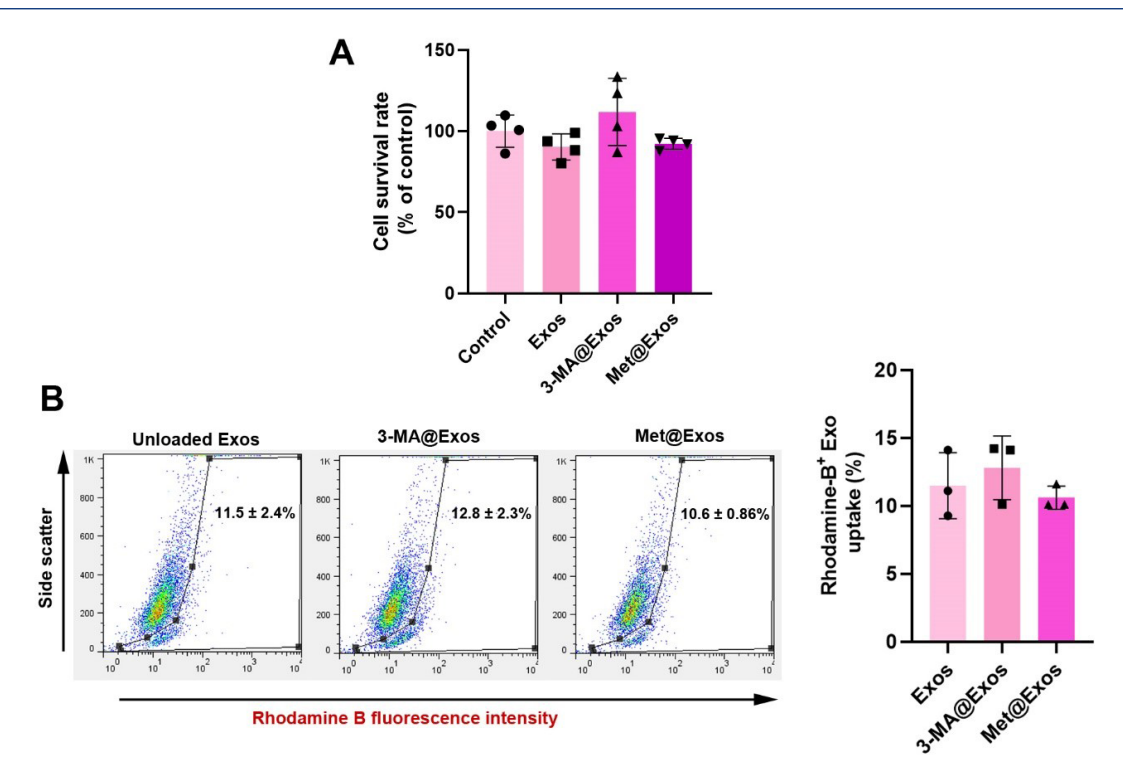


Fig. 3. Monitoring the survival rate of MDA-MB-231 cells after being exposed to Exos, 3-MA@Exos, and Met@Exos for 48 hours using the MTT assay (A; n=4). Internalization rate of Rhodamine B-labeled Exos by human MDA-MB-231 cells after 4 hours (B). Data indicated the lack of statistically significant differences in the percentage of cells with internalized Exos compared to the control (unloaded) Exos. One-way ANOVA with Tukey post hoc analysis (n=3).

properties or intoxication on human MDA-MB-231 cells. Flow cytometry analysis revealed that the loading of 3-MA and/or Met did not affect the internalization rate in human Exos in human MDA-MB-231 cells (Fig. 3B). Data revealed that the percentage of MDA-MB-231 cells with internalized Rhodamine B-labeled Exos reached 12.8 \pm 2.3 and 10.6 \pm 0.86% compared to the control Exos group (11.5 \pm 2.4%; P > 0.05) after 4 hours in *in vitro* conditions. These data confirmed the lack of detrimental effects of loading techniques in Exo uptake by MDA-MB-231 cells (Fig. 3B).

Autophagy status

Western blotting

The autophagy response was monitored using western blotting in MDA-MB-231 cells 48 hours after being treated with 5 μg/mL Met or 10 μM 3-MA. In this regard, protein levels of Beclin-1, LC3, and p62 were measured. Data showed the increase of Beclin-1 in 3-MA, 3-MA@ Exos, Met, and Met@Exos groups compared to the Exos and non-treated control, indicating the initiation of autophagy response (Fig. 4A). Along with these changes, total LC3 contents were also heightened in 3-MA, 3-MA@ Exos, Met, and Met@Exos groups as compared to the non-treated control. Of note, this increase was less in the group that received Exos alone, and maximum effects were shown in the cells that were treated with free 3-MA (Fig. 4A). Full-length blots are provided as Fig. S2. The stimulation of LC3 indicates the activation of autophagic

flux in MDA-MB-231 cells after 48 hours. Monitoring the intracellular levels of p62 indicated a prominent reduction in Met, Met@Exos, and Exos groups, resulting in the completion of autophagy response, while higher levels of p62 were achieved in control, 3-MA, and 3-MA@ Exos groups. These features confirmed that free 3-MA, Met, and Exos bearing 3-MA and Met can initiate the autophagy response via the induction of Beclin-1 and an increase of LC3, while completion of the autophagy response is significant in the groups that received free Met, Met@Exos, or Exos alone.

IF staining

Using IF staining, the cytoplasmic LC3*puncta, a marker of autophagosomes, were imaged in the different experimental groups (Fig. 4B). Similar to data from the western blot panel, it was shown that the intensity of green-colored LC3 puncta was increased in 3-MA, 3-MA@Exos, Met, and Met@Exos groups compared to the Exos and control groups (Fig. 4B). It seems that the cells that received free 3-MA alone had a higher signal of fluorescence related to LC3 contents, and this increase in descending order in Met, 3-MA@Exos, and Met@Exos groups. It can be said that the modulation of autophagy by free Met, 3-MA, or drug-loaded Exos can influence the cytoplasmic content of LC3, indicating the potential impact on autophagy flux.

PCR array analysis

To indicate the impact of 3-MA, Met, 3-MA-, and Met-

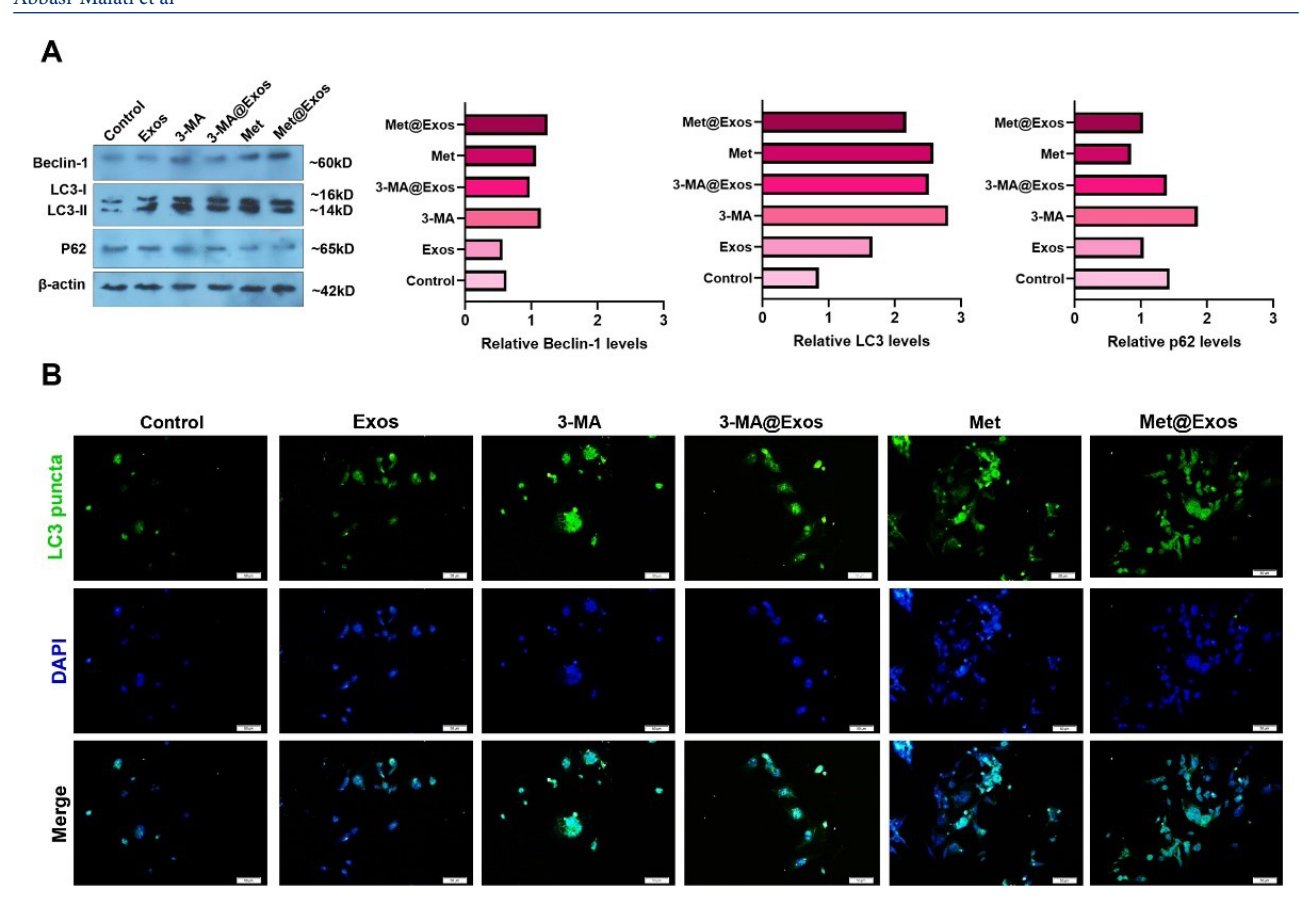


Fig. 4. Monitoring the autophagy status in MDA-MB-231 cells using western blotting and immunofluorescence staining after 48 hours. Western blotting indicated the changes in the levels of Beclin-1, LC3, and p62 inside the MDA-MB-231 cells after being treated with 5 μg/mL Met, 10 μM 3-MA, or Met-, 3-MA-loaded Exos (A; data were obtained from three pooled samples). The blots were cropped and presented in panel A. A similar trend was achieved in intracellular levels of green-colored LC3*puncta in different experimental groups using IF staining (B).

loaded Exos on different effectors related to autophagy signaling pathways, PCR array analysis was conducted (Tables S1 and S2, and Fig. 5). Data indicated the upregulation, and/or down-regulation of different genes in the presence of 3-MA, Met, 3-MA-, and Met-loaded Exos in MDA-MB-231 cells after 48 hours. Treatment of MDA-MB-231 cells with Met or Met-loaded Exos can increase the expression of genes related to autophagic vacuole formation and vacuole targeting in which genes including AMBRA1, ATG12, ATG16L1, ATG4A, ATG4B, ATG5, ATG9A, BECN1, GABARAP, GABARAPL1, GABARAPL2, MAPILC3A, MAPILC3B, RGS19, and *ULK1* were up-regulated as compared to the non-treated cells (Table S2). While the expression of ATG4C, IRGM, and WIPI1 was different in the Met and Met@Exos groups. The expression of genes such as ATG12, ATG4A, ATG4B, ATG4C, ATG4D, ATG5, GABARAPL1, MAP1LC3A, and RGS19 was similarly down-regulated in 3-MA and 3-MA@ Exos groups. These data indicated that Met and Met@ Exos can promote the formation of autophagic vacuoles, and most of these genes were inhibited in the presence of free 3-MA or 3-MA@Exos. Of note, the transcription of genes related to protein transport, such as ATG10, ATG16L2, ATG4B, ATG4C, ATG7, and GABARAPL1,

was down-regulated in 3-MA and 3-MA@Exos treated cells compared to the control group. On the contrast, the expression of ATG4A, ATG4B, ATG7, ATG9A, GABARAP, GABARAPL1, GABARAPL2 remained unchanged or stimulated in Met, and Met@Exos groups (Table S2). Based on the obtained data, the expression of autophagosome-lysosome linkage genes, mainly LAMP1, was up-regulated in Met and Met@Exos groups, and down-regulated in 3-MA or 3-MA@Exos. Other genes from the same signaling axis, such as DRAM1, GABARAP, and NPC1, exhibited different expression patterns. Data confirmed that 3-MA and 3-MA@Exos can influence the ubiquitination process via the down-regulation of ATG7 and concomitant expression of ATG3 (Table S2). The expression of HDAC6 did not show a similar pattern in these groups. Based on the data, the expression of ATG3 and ATG7 was increased in Met-treated groups with superior effects in the presence of Met@Exos. Likewise, the effectors associated with chaperone-mediated autophagy, including HSP90AA1 and HSPA8, were also stimulated in Met and Met@Exos groups, while these factors were inhibited or unchanged in 3-MA and 3-MA@Exos groups. We also noted that most of the genes that behave as co-regulators of autophagy & apoptosis

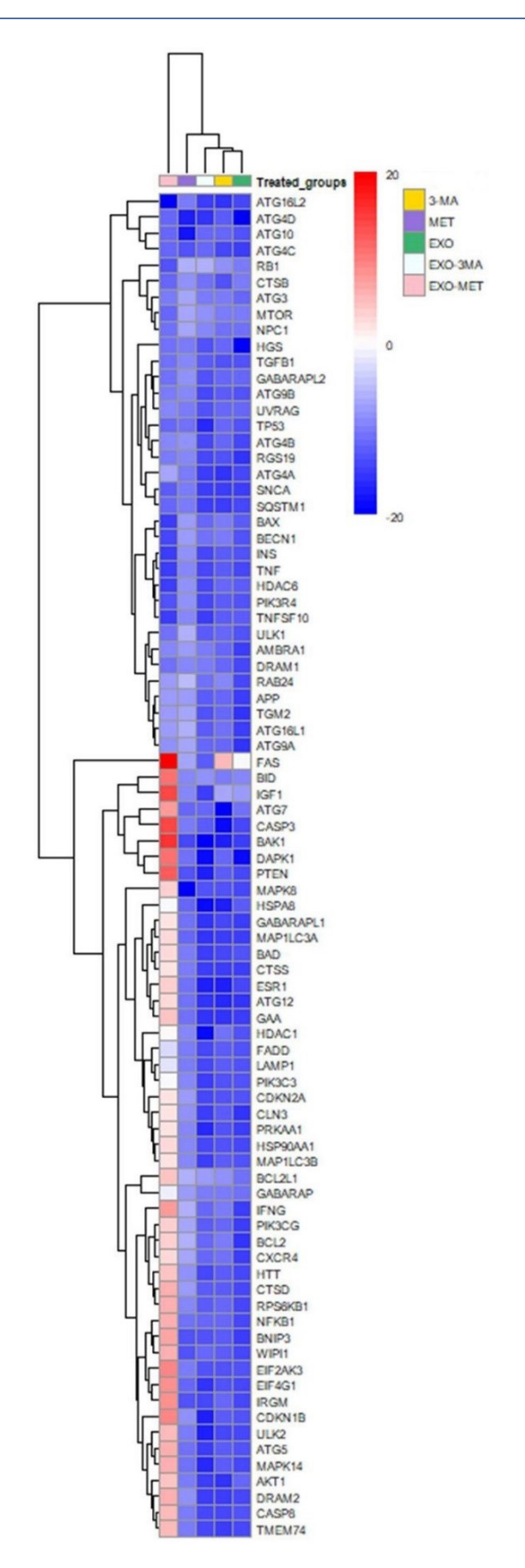


Fig. 5. Clustergram illustration of autophagy genes in BC MDA-MB-231 cells treated with Exos, Met, 3-MA, Met@Exos, and 3-MA@Exos for 48 hours (n=3). The red and green areas indicate the up-regulation and down-regulation, respectively.

were up-regulated in Met, and Met@Exos groups with concomitant downregulation in other groups (Tables S1 and S2). The data showed that pro-apoptotic genes such as AKT1, APP, ATG12, BAD, BID, CASP3, CASP8, CDKN2A, CDKN1B, FADD, FAS (TNFRSF6), HDAC1, HTT, IFNG, PRKAA1, TGM2 were significantly upregulated in Met, and Met@Exos groups. Anti-apoptotic genes such as BCL2, BCL2L1 (BCLXL), CLN3, CXCR4, EIF2AK3, IGF1, PIK3CG, and TGFB1 were increased simultaneously in Met, and Met@Exos groups. Of note, most of the pro- and anti-apoptotic factors were downregulated in Exos, 3-MA, and 3-MA@Exos groups as compared to the control MDA-MB-231 cells, Met, and Met@Exos groups. These data indicate that several genes related to the autophagy signaling pathway are activated in the presence of free Met or Met-loaded Exos, while most of these genes were inhibited when MDA-MB-231 cells were exposed to 3-MA or 3-MA-loaded Exos. Thus, 3-MA and Met can influence the autophagy signaling pathway, free from or after being loaded onto the Exos.

Autophagy modulation influenced tumor cell migration and paracrine angiogenesis capacity

Here, the possible effects of autophagy modulation were monitored on MDA-MB-231 cell migration and paracrine angiogenesis properties after being incubated with free 3-MA, Met, or 3-MA and Met-loaded Exos for 48 hours (Fig. 6). Data indicated that 48-hour treatment of BC MDA-MB-231 cells with Exos stimulated the number of migrating cells compared to the control group (Fig. 6A-B). Unlike the Exos group, the migration rate was not statistically significant in the 3-MA group as compared with control cells. The incubation of cells with 3-MAloaded Exos can increase the migration rate compared to the control group. A similar pattern was evident in Met and Met@Exos groups after 48 hours, with the most prominent effects in the Met@Exos group. However, these effects were not statistically significant between the Exos, 3-MA, Met, 3-MA@Exos, and Met@Exos groups. These data show that autophagy modulation can influence the migration of MDA-MB-231 cells using free 3-MA, Met, or 3-MA@Exos, and Met@Exos.

We also monitored the migration of HUVECs after being exposed to the secretome of MDA-MB-231 pretreated with 3-MA, Met, 3-MA@Exos, and Met@Exos (Fig. 6C). Of note, pre-treatment of MDA-MB-231 cells with Exos alone did not influence the paracrine angiogenesis capacity. Data revealed a lack of statistically significant differences in terms of HUVEC migration in 3-MA-, 3-MA@Exos-treated MDA-MB-231 cells as compared to the non-treated control cells. In the Met@Exos, but not Met, group, the number of migrated cells was increased compared to the experimental groups (Fig. 6C). Notably, these changes were not significant when compared to the Met group. These data confirmed that

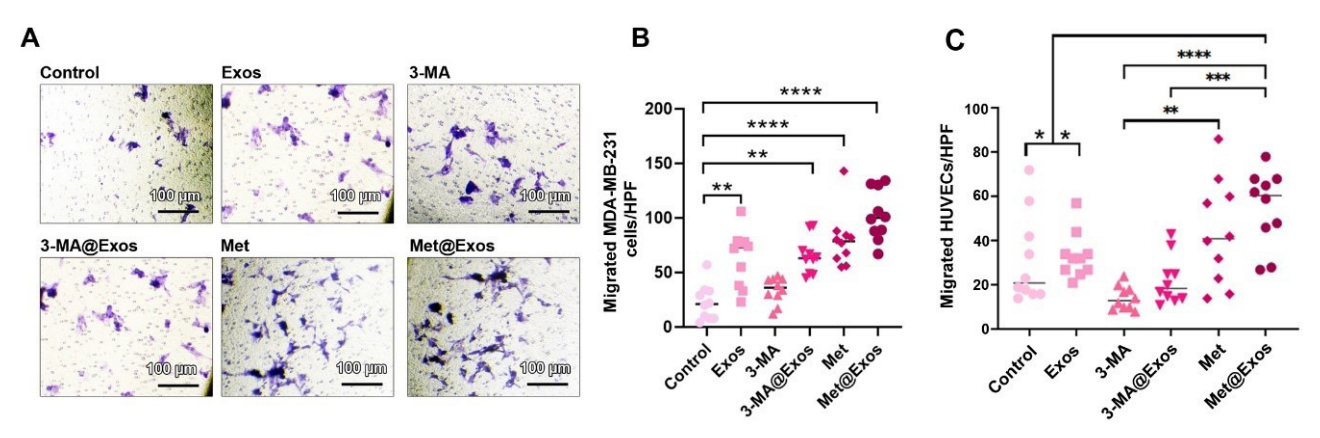


Fig. 6. Transwell inserts migration assay (A-C). Monitoring the migration of MDA-MB-231 cells 48 hours after treatment with Exos, Met, Met@Exos, 3-MA, and 3-MA@Exos (A-B; n=9). HUVECs migration rate incubated with MDA-MB-231 cells pre-treated with Exos, Met, Met@Exos, 3-MA, and 3-MA@Exos (C; n=10). One-way ANOVA with Tukey post hoc analysis. ** P<0.01, *** P<0.001, and ****P<0.0001.

the stimulation of autophagy via drug-loaded Exos can lead to the angiogenesis response mainly via enhancing HUVECs migration.

Angiogenesis properties

The expression of different genes, IL-8, CDH5, TIMP3, ERBB2, HIF1A, IFNA1, MMP2, VEGFA, NOTCH4, IL-1B, PECAM1, and IL-6 were monitored using real-time PCR analysis (Fig. 7A, and Table 2). Based on the obtained data, treatment of MDA-MB-231 cells with Exos led to the down-regulation of almost all included genes compared to the control group. In the 3-MA-treated cells, the expression of MMP2, VEGFA, NOTCH4, IL-8, and TIMP3 was reduced, while the transcription of genes such as IL-1 β and PECAM1 was increased as compared to the control cells (Fig. 7A and Table 2). A relatively similar trend was reported in the cells incubated with 3-MA@ Exos for 48 hours. The expression of IL-8, TIMP3, ERBB2, MMP2, VEGFA, NOTCH4, PECAM1, and IL-6 was also

diminished in the Met@Exos groups with concomitant up-regulation of IL1B, and PECAM1. The ELISA assay showed that the levels of VEGF were diminished in 3-MA-treated cells, similar to the genomic panel (Fig. 7B). The down-regulation of VEGF was also reported in the Met and Met@Exos groups. These data indicated the significant reduction of angiogenesis-related factors such as VEGF in BC cells after the modulation of autophagy response (Fig. 7B). Both induction and stimulation of autophagy can influence the angiogenesis factors *in vitro*.

Alg/Gel microspheres provided a suitable niche for BC tumoroid cells

In the present work, Alg/Gel microspheres were used for the development of BC tumoroids. Bright-field images indicated the relatively even distribution of BC tumoroids inside the microspheres (Fig. 8A; panel left). Based on our calculation of the mean size of Alg/Gel microspheres reached $413.63\pm42.24~\mu m$ in cell-laden microspheres

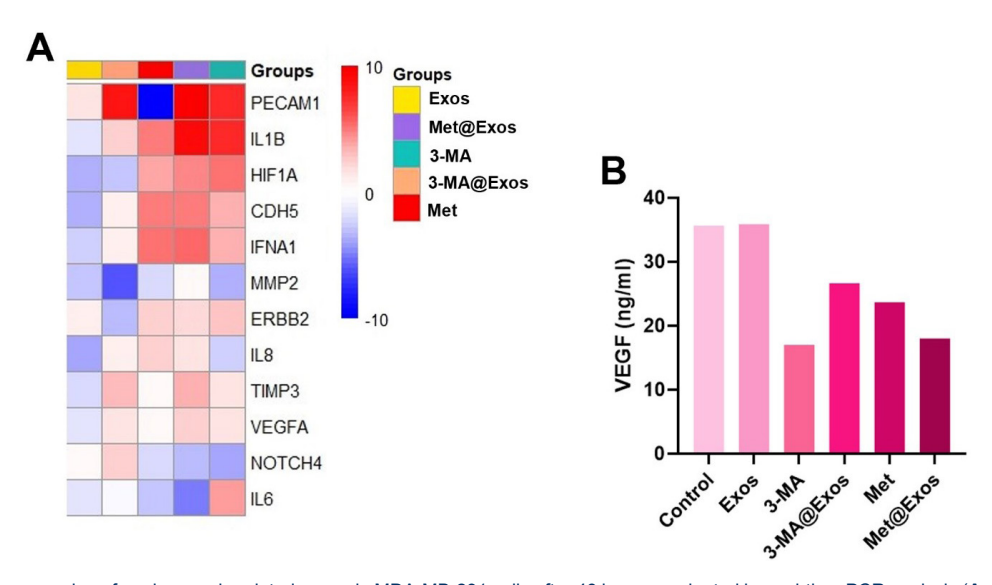


Fig. 7. Clustergram mapping of angiogenesis-related genes in MDA-MB-231 cells after 48 hours, evaluated by real-time PCR analysis (**A**; n=3). Measuring protein levels of VEGF using ELISA (**B**; data were obtained from three pooled samples).

Table 2. Monitoring the angiogenesis pathway in MDA-MB-231 cells after 48 hours

Genes	Exos	ЗМА	3MA@Exos	Met	Met@Exos
IL8	-13.27	-6.96	-3.46	-2.23	-3.03
CDH5	-10.56	-1.60	-3.34	1.24	1.25
TIMP3	-6.45	-2.89	-1.75	-3.76	-1.57
ERBB2	-3.20	-1.93	-8.94	-2.35	-2.53
HIF1A	-9.92	1.32	-8.06	-1.37	1.09
IFNA1	-7.52	-1.60	-3.36	1.32	1.49
MMP2	-8.63	-10.13	-30.27	-6.82	-3.86
VEGFA	-5.94	-2.91	-2.99	-3.76	-2.25
NOTCH4	-4.03	-12.73	-2.25	-6.50	-8.88
IL1B	-5.74	3.51	-2.25	1.19	4.92
PECAM1	-2.75	3.43	4.11	-70.03	6.02
IL6	-5.50	-1.25	-4.26	-8.46	-18.25
HPRT1	1.00	1.00	1.00	1.00	1.00

Fold-change values in human MDA-MB-231 cells treated with free Met and 3-MA, or Met-, and 3-MA-loaded Exos were calculated using the $2^{-\Delta \Delta Ct}$ methods related to the non-treated control group. Differences in expression more than twofold were accepted as the cut-off value (n = 3).

when compared to the cell-free groups $(397.94\pm74.07 \, \mu m; \, Fig. \, 8A; \, panel \, right)$. Data indicated that the cell-laden and cell-free samples had stability over 14 days. SEM images indicated the existence of pores in the structure of Alg/Gel microspheres (Fig. 8B; left panel, yellow arrows). Data showed that cells can attach to the backbone of Alg/Gel microspheres and acquire flattened morphologies (Fig. 8B; middle and right panels; yellow arrows). MTT assay confirmed the cytoprotective features of Alg/Gel microspheres on BC tumoroids treated with Met for 48 hours when compared to the 3-MA group (P < 0.05; Fig. 8C). No statistically significant differences were found in terms of cell survival in 3-MA-treated microspheres compared to the control microspheres.

Met increased cell density of BC tumoroids inside Alg/ Gel microspheres

Using H & E staining, the cell density was studied in each microsphere after being treated with Met or 3-MA for 48 hours (Fig. 8D). Data showed the increase of cell density in Met-treated Alg/Gel microspheres when compared to the 3-MA and control (P<0.05; Black arrows). These data show that Met can increase the number of BC tumoroids inside Alg/Gel microspheres.

Met increased the metastasis and tumor formation of cell-laden microspheres in vivo

Orthotopic mammary gland transplantation of BC tumoroids encapsulated inside Alg/Gel microspheres showed that Alg/Gel microspheres can be detected in the control and 3-MA groups (Fig. 8E). In the control group, some cells could be detected inside the microsphere

parenchyma, while cells were barely detected inside the Alg/Gel microspheres pre-treated with 3-MA. In both groups, the microspheres are enclosed by a thin fibrotic layer. In contrast, the microspheres were degraded in the Met group, and their remnants were detected as dark purple clumped masses devoid of cells. It seems that these cells migrated into the neighboring tissues and generated metastatic foci with a lobular form (Fig. 8E). These features indicate that the treatment of encapsulated BC tumoroids with Met can increase the possibility of tumor cell metastasis into the mammary gland and the generation of metastatic foci.

Discussion

As a common belief, autophagy response is a fundamental phenomenon in the control of dynamic growth and bioactivity of tumor cells, especially CSCs.34 More interestingly, autophagy with a dual role in tumor cells and CSCs can function as pro-survival and tumoricidal factors.35-37 For example, it was suggested that autophagy inhibition and/or overactivity can influence the angiogenesis rate and vascularization into the tumor parenchyma in different pathological conditions, highlighting the critical role of autophagy machinery in tumor biology.38,39 Recent studies have highlighted that over-activation and inhibition of autophagy can result in opposing effects in the context of tumor angiogenesis. For instance, autophagy activation in breast cancer cells has been associated with enhanced VEGF secretion and promotion of angiogenesis,40 whereas long-term or excessive induction of autophagy has been reported to impair vascular maturation and attenuate tumor perfusion.41 Similarly, it has been shown that autophagy stimulation in CD146+ cells can drive their differentiation into endothelial-like phenotypes,42 while inhibition of autophagy using 3-MA significantly reduced endothelial cell sprouting and in vitro tubulogenesis.43 These findings emphasize that autophagy exerts context- and dose-dependent roles in regulating angiogenesis within the tumor microenvironment.44,45 Due to the lack of knowledge related to the autophagy-angiogenesis relationship in cancer biology, this study aimed to address how and by which mechanisms autophagy modulation can inhibit/stimulate the angiogenesis response in human BC cells. MDA-MB-231 cells contain a large CD44+/CD24population with stemness features.46 For this purpose, two autophagy modulators, free Met and 3-MA or Met-, and 3-MA-loaded Exos were used for the regulation of autophagy.

We aimed to use human blood Exos as bioshuttles for the delivery of 3-MA and Met into the target MDA-MB-231 CSCs. Based on the present data, it was found that the loading efficiency of Met in Exos was 23%. Consistent with our results, Zhan et al reported an approximate loading efficiency of 20.7% for Met in blood

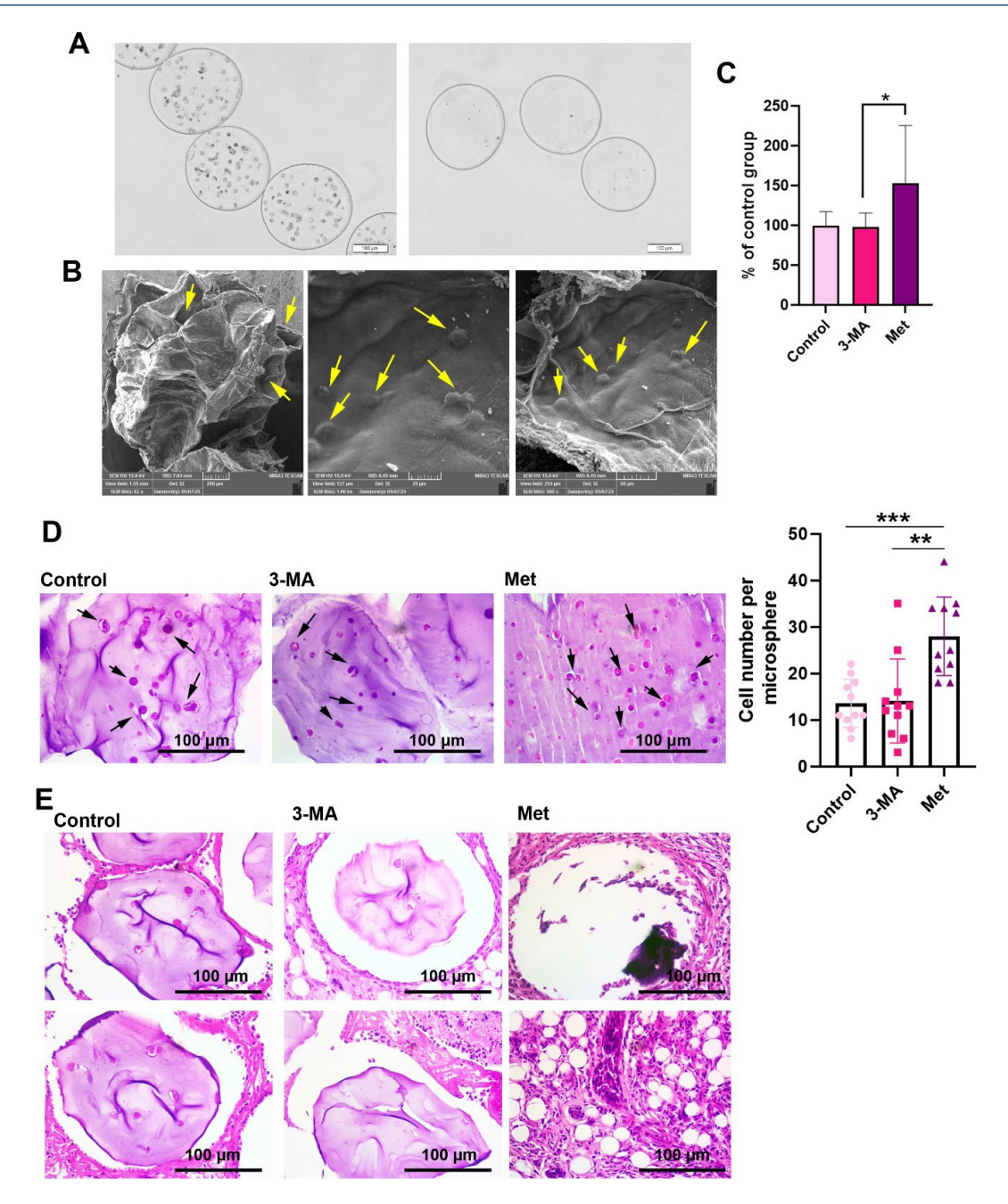


Fig. 8. Development of BC tumoroids inside the Alg/Gel microspheres crosslinked by CaCl₂. Bright-field images indicated the distribution of HUVECs, MDA-MB-231 cells, and HFFF2 cells inside the microspheres (**A**: Left panel: cell-laden microspheres; Right panel: cell-free microspheres). SEM images of Alg/Gel microspheres. Data showed the existence of pores in the structure of Alg/Gel microspheres (**B**; Left panel). Cells can attach to the backbone of Alg/Gel microspheres and acquire relatively flattened morphologies (**B**: middle and right panels). MTT assay of BC tumoroids inside the Alg/Gel microspheres after 48 hours (**C**: n=13). Monitoring cell density in Alg/Gel microspheres after 48 hours in the presence of Met and 3-MA in *in vitro* conditions (**D**; n=11). Met increases the mean cell number in Alg/Gel microspheres compared to the control and 3-MA groups. Histological examination of mice mammary glands using orthotopic transplantation of human BC tumoroids inside the Alg/Gel microspheres after two weeks (**E**). One-way ANOVA with Tukey post hoc analysis. *** P < 0.05; *** P < 0.01, and ****P < 0.001.

Exos.⁴⁷ While exogenous 3-MA loading in human Exos reached 64%. One reason for the difference in the loading capacity of Met and 3-MA in Exos can be related to the chemical structure of these compounds. Considering the chemical formula, Met hydrochloride, as used in this study, is more hydrophilic and exhibits organic cations at the physiological pH values as compared with the 3-MA.⁴⁸ Consistent with our observations, other groups

have demonstrated that the chemical nature of the cargo strongly influences the encapsulation efficiency. For example, hydrophilic molecules such as Met exhibit significantly lower loading efficiency compared with more hydrophobic drugs, due to their limited compatibility with the lipid bilayer of Exos.²⁹ This is consistent with our finding that 3-MA achieved a markedly higher loading percentage than Met. Moreover, drug—

membrane interactions have been highlighted as critical determinants for the stability of encapsulation.²⁹ These data support the notion that the higher loading of 3-MA versus Met is largely based on chemical compatibility with the exosomal membrane. Our data also indicated that the sonication process and loaded drugs did not affect the internalization rate of labeled Exos in MDA-MB-231 cells in the early 4 hours, as compared to the control Exo group. It has been proposed that Exos and other EV types can enter the recipient cells via different mechanisms, such as endocytosis, direct fusion with the cell membrane, micropinocytosis, phagocytosis, and lipid rafts.¹⁸ If it is assumed that the loading protocol inhibits the uptake of Exos by a specific route or makes a slight change in the structure of Exos, the existence of other mechanisms can compensate for the entry of Exos into the MDA-MB-231 cells. Thus, we propose that due to the different modes of Exo internalization in the recipient cells, non-statistically significant differences were obtained.

It was also noted that treatment of MDA-MB-231 cells with Met and Met@Exos led to the activation of autophagy (Beclin-1, LC3↑, and p62↓) after 48 hours. PCR array also indicated the upregulation of different autophagy effectors in Met and Met@Exos groups. Despite the increase of LC3 and Beclin-1 levels in 3-MA and 3-MA@ Exos groups, the increase of p62 showed an impaired autophagy response in these groups. It is thought that the close interaction of p62 and LC3 provides a platform for the degradation of ubiquitinated cargoes by autophagy.⁴⁹ PCR array analysis revealed the significant and slight down-regulation of MAP1LC3A and B in 3-MA-treated groups compared to the control cells. Along with these changes, the expression of SQSTM1/p62 was also reduced in these groups. The reduction of GABARAPL1 and LAMP1 indicated an impaired autophagy flux and fusion with lysosomes in the MDA-MB-231 cells in the presence of free 3-MA or loaded 3-MA in Exos.⁵⁰ The reduced expression of specific genes such as HSP90AA1 and HSPA8 in 3-MA-treated groups confirmed the inhibition of chaperone-mediated autophagy, while the expression of these genes was significantly increased in Met-treated groups.51 These findings are in close alignment with past reports. As examples, 3-MA inhibition of autophagy flux by reducing LC3-II expression and lysosomal fusion impairment with consequent p62 accumulation and faulty autophagosome maturation have been shown.^{50,52} On the contrary, activating AMPK and suppressing mTOR results in Met-mediated induction of autophagy with elevated LC3-II and Beclin-1 levels.⁵³ Correspondingly, the lack of recruitment of autophagy proteins, including GABARAPL1 and LAMP1, upon 3-MA administration was shown to confirm a partial maturation deficiency in autophagosomes.⁵⁰ To support this, chaperone-mediated autophagy modifications were also noted with HSP90AA1 and HSPA8 downregulation in 3-MA-treated groups,

while Met significantly increased their expression.54 Moreover, it is shown previously that Met can stimulate autophagy and allow protective stress responses in triple-negative breast cancer cells, in keeping with our observations.55 Taken together, these data indicate that treatment of MDA-MB-231 cells with the free 3-MA or 3-MA@Exos can lead to the suppression of autophagy response at different molecular levels. In contrast, the expression of various genes associated with autophagy machinery was induced in the presence of Met. Our data indicate that Exos loaded with Met and/or 3-MA are relatively suitable bio-shuttles in the modulation of autophagy response in human MDA-MB-231 cells. In line with present data, previous research has confirmed the Exos as effective nanocarriers in the delivery of chemicals and biological molecules for different regenerative purposes.56

Genomic data also indicated the up-regulation and down-regulation of co-regulators of autophagy & apoptosis in different experimental groups. Most of these genes were stimulated in the Met and Met@Exos groups. It seems that these changes were compensatory mechanisms in response to the autophagy modulation. Even though the activation of pro-apoptosis genes did not yield reduced cell survival, as indicated by the MTT assay. Thus, it can be said that the alteration of autophagy effects alters the expression of apoptosis genes as well. Recent studies provide strong evidence supporting these observations. For example, it has been reported that induction of autophagy can upregulate pro-apoptotic markers without significantly reducing cell viability, suggesting that autophagy may act as a compensatory survival mechanism in breast cancer cells.⁵⁵ Similarly, Met treatment was shown to activate autophagy while simultaneously priming apoptotic pathways, yet this activation did not necessarily culminate in immediate cell death, which is consistent with our results.⁵⁵ In addition, inhibition of autophagy by 3-MA has been associated with disruption of apoptotic signaling crosstalk and altered gene expression patterns, although without marked shortterm effects on cell survival. 50,51 Collectively, these findings reinforce the concept that the autophagy-apoptosis interplay is highly context-dependent, functioning more as a dynamic regulatory balance than a simple survivalversus-death switch.57

It was also shown that the migration rate of MDA-MB-231 cells was increased when exposed to Met and Met@Exos when compared to the control and 3-MA groups. Autophagy response can increase cell migration via engaging several mechanisms.^{58,59} One possible mechanism would be that the changes in fatty acid composition and generation of lamellipodia and tunneling nanotubes are stimulated in the presence of an autophagy response, resulting in relatively suitable morphological adaptation, which can help the cell to move easily to

different sites inside the body.⁵⁹ The maximum migration rate was evident in MDA-MB-231 cells treated with Met@ Exos. Cao et al indicated that autophagy can increase the migration of normal fibroblasts by lung cancer cells via concomitant induced epithelial-mesenchymal transition and an increase of IGF-2, leading to active cell migration.⁵⁸ These features reduce the attachment of tumor cells to the supporting extracellular matrix (ECM) and induce migration capacity.⁵⁷ Besides, autophagy activation can stimulate triple negative BC cells, like MDA-MB-231 cells, via nuclear translocation of oncogenic effectors such as YAP belonging Hippo signaling pathway.⁵⁷ The reduction of migration rate in 3-MA-treated groups can be related to the suppression of Beclin-1 and MAP1LC3, confirmed by PCR array analysis. These factors can stabilize the β1 integrin-related signaling cascade. The inhibition of the β 1 integrin signaling pathway leads to the deactivation of the urokinase-type plasminogen activator system, which is critical in cell migration and metastasis.⁵⁷ The existence of statistically significant differences in the number of migrated cells between the 3-MA@Exos compared to control groups would be presumably related to the existence of genetic traits and proteomic features inside the Exo lumen with the potential to alter the cell migration capacity, as such properties were evident in the Exos group as well. In line with these claims, the migration rate was reduced in the 3-MA group.

We also monitored the angiogenesis potential of BC MDA-MB-231 cells after activation and/or inhibition of autophagy response. Despite the increase in metastasis properties, the induction of autophagy led to a reduction of VEGF factor in the Met and Met@Exos groups compared to the control and Exos groups. These values were prominently reduced in the 3-MA group. In contrast, autophagy modulation increases the expression of PECAM (CD31) in 3-MA, 3-MA@Exos, and Met@ Exos groups, except Met-treated cells. These features confirmed the trans-differentiation of MDA-MB-231 cells into the endothelial lineage. Other angiogenesisrelated genes were reduced in 3-MA- and Met-treated groups. As a common belief, autophagy activation can promote tumor development and expansion via the stimulation of angiogenesis.⁴⁵ Even though both inhibition and stimulation of autophagy can promote the expression of endothelial cell-like factors, such as PECAM. In a previous study, we indicated that autophagy stimulation in CD146+cells can promote endothelial lineage, cardiomyocyte, and pericyte differentiation in vitro when compared to the hydroxychloroquine-treated cells.42 In the present study, it was noted that autophagy modulation can inhibit the majority of angiogenesisrelated factors, except for some genes such as PECAM. In the Met and Met@Exos groups, the expression of TGF-β reached 4.5- and 2.2-fold when compared to the control cells. It has been shown that TGF-β can physically interact

with the Neuropilin-1 receptor, leading to the suppression of angiogenesis capacity. 40 The lack of significant changes in HIF-1a expression in these groups may point to the fact that activation of autophagy signaling in hypoxic conditions results in better angiogenesis outcomes.44 Of course, it should not be forgotten that excessive autophagy response not only does not promote vascularization potential but can also contribute to impaired angiogenesis.41 However, the reduction of angiogenesis in 3-MA-treated cells is highly associated with the inhibition of different effectors related to the autophagy signaling pathway. Recent data indicated that autophagy inhibition can blunt the angiogenesis response in terms of in vitro tubulogenesis and endothelial cell sprouting.42 These results are consistent with recent studies that highlight the multifaceted and context-dependent role of autophagy in regulating angiogenesis. Indeed, for instance, stimulation of autophagy in breast cancer cells was shown to inhibit VEGF secretion in an AMPK-dependent manner,40 which is consistent with our observed reduced VEGL levels in our Met-treated groups. On the contrary, inhibition of autophagy by 3-MA was shown to prevent endothelial sprouting and in vitro tube formation, which is in line with our noted disabled angiogenesis in 3-MAtreated animals.43 Moreover, it has been speculated that chronic or excessive autophagy activation might counterintuitively inhibit angiogenesis by evoking endothelial cell dysfunction or cell death by apoptosis, which is not in contradiction with our noted result that overactivation does not enhance pro-vascularization.⁴¹ The combined results indicate that autophagy fulfills a bifunctional regulatory function in angiogenesis: whereas mild stimulation may stimulate endothelial-like transdifferentiation (e.g., upregulation of PECAM/CD31),45 pharmacologic inhibition and excessive overactivation would ultimately lead to vascular dysfunction.44

We also found that treatment of encapsulated MDA-MB-231 cells, HUVECs, and HFFF-2 cells inside Alg/ Gel microspheres with Met led to increased survival rate compared to the control and 3-MA groups and free MDA-MB-231 cells. The 3D culture system with Alg/ Gel microspheres bearing HUVECs, MDA-MB-231 cells, and HFFF-2 cells can recapitulate the relatively in vivo conditions. The enhanced survival rate is possibly due to the 3D microenvironment provided by Alg/Gel microspheres. The existence of Gel within the Alg network provides the essential clues and motifs required for the stimulation of tumor cells and other cell types. 60,61 Besides, the assembling of three cell lineages inside the Alg/Gel microspheres can support the vital signals to maintain the dynamic growth of tumor cells or vice versa in response to autophagy modulation using different chemicals.⁶² Commensurate with these data, the histological examination confirmed that the local density of cells increased in Met-treated microspheres compared to other groups. Whether BC

cells, HUVECs, or HFFF-2 cells responded to autophagy stimulation needs further investigation. However, the inhibition of autophagy response using 3-MA did not alter the survival rate compared to the encapsulated BC tumor cells inside the Alg/Gel microspheres. More interestingly, the orthotopic injection of BC tumoroids into female mice led to the expansion of tumor-like structures to the neighboring tissue, while in the control and 3-MA groups, the structure of Alg/Gel microspheres was relatively intact, harboring few cells. The integrity of supporting Alg/Gel microspheres was entirely lost, and cells migrated into the juxtaposed tissue. One reason would be that autophagy stimulation acts as an oncogenic factor in the tumorigenesis of BC tumoroids inside the Alg/Gel microspheres.⁶³ The histological examination revealed the generation of lobular structures inside the mammary gland parenchyma juxtaposed to the injection sites. The loss of the Alg/Gel matrix can also be associated with enhanced metastatic behavior of tumor cells.64 While the number of encapsulated cells per Alg/Gel microspheres was reduced in the 3-MA group.65 Taken together, the stimulation of autophagy can promote encapsulated tumor cell dynamic growth and metastasis to the juxtaposed niches after transplantation. These results are consistent with previous studies which show 3D Alg/Gel scaffolds produce a microenvironment favorable for tumor support by mimicking extracellular matrix signaling and up-regulating cancer cell viability, ultimately benefiting the in vitro survival of breast cancer cells.⁶⁶ Similarly, it is reported that breast cancer spheroids cultured in GelMA-based hydrogels show enhanced proliferative and invasive capacity, which is consistent with our finding of enhanced cell density in Met-treated microspheres.⁶⁷ On the contrary, inhibition of autophagy by 3-MA administration is found to result in decreased proliferation and decreased viability in 3D tumor spheroids, which is consistent with our result showing 3-MA treatment impaired the viability of breast cancer cells.⁶⁴ Moreover, the in vivo disintegration of Alg/ Gel microspheres followed by local invasion of BCs is consistent with past research which shows activation of autophagy facilitates extracellular matrix destruction and metastatic niche formation.63

Moreover, the in vivo disintegration of Alg/Gel microspheres followed by local invasion of breast cancer cells is consistent with past research, which shows that activation of autophagy facilitates ECM destruction and metastatic niche formation.

Conclusion

The current data underscore the putative role of autophagy regulation in the angiogenesis capacity of triple-negative human BC cells. The autophagy activator/inhibitor was successfully introduced to the BC MDA-MB-231 cells using Exos as valid bioshuttles. Data also confirmed the

Research Highlights

What is the current knowledge?

 The role of autophagy has been proven in the bioactivity of tumor cells.

What is new here?

- Autophagy inhibition/stimulation can influence the activity of breast cancer cells.
- Autophagy activation/inhibition led to changes in angiogenesis potential.
- Activation of autophagy promoted cell metastasis in in vivo conditions.

relatively congruent changes in drug-loaded Exos groups when compared to matched control groups, indicating Exos as a smart delivery vehicle for the modulation of autophagy. We also found that autophagy modulation can alter the migration capacity and angiogenesis response in these cells, which can be crucial in the control of tumor cell metastasis and expansion in *in vivo* conditions. *In vivo* data confirmed that stimulation of autophagy can trigger BC tumoroids expansion and metastasis into the mammary gland in mice receiving orthotopic xenogeneic implantation. It is suggested that the present data underscore the potential of targeting autophagic pathways and Exo-mediated processes, someday being able to enhance therapeutic strategies in BC patients some days in the near future.

Acknowledgments

We thank the personnel of the Faculty of Advanced Medical Sciences and the Stem Cell Research Center for their help and guidance. The authors declare that they have not used AI-generated work in this manuscript.

Authors' Contribution

Conceptualization: Reza Rahbarghazi. Data curation: Zeinab Aliyari Serej. Funding acquisition: Reza Rahbarghazi.

Investigation: Zahra Abbasi-Malati, Çığır Biray Avci, Parisa Khanicheragh, Zeinab Aliyari Serej, Maryam Sabour Takanlou, Leila Sabour Takanlou

Methodology: Zahra Abbasi-Malati, Çığır Biray Avci, Parisa Khanicheragh, Zeinab Aliyari Serej, Maryam Sabour Takanlou, Leila Sabour Takanlou, Seyed Ghader Azizi, Zohreh Sanaat, Nafiseh Didar Khosrowshahi, Hassan Amini, Rasoul Hosseinpour.

Project administration: Reza Rahbarghazi.

Supervision: Reza Rahbarghazi.

Validation: Nafiseh Didar Khosrowshahi, Hassan Amini.

Visualization: Çığır Biray Avci.

Writing-original draft: Zahra Abbasi-Malati. Writing-review & editing: Reza Rahbarghazi.

Competing Interests

Authors declare that there are no known conflicts of interest.

Ethical Approval

This study was done according to the World Medical Association Declaration of Helsinki guidelines. The animal experiments were done based on the guidelines of "The Care and Use of Laboratory Animals" (NIH Publication No. 85-23, revised 1996). The study was also registered as titled "Modulation of autophagic response on breast cancer stem

cell angiogenic properties using exosomes" under an approval code of IR.TBZMED.VCR.REC.1401.392 from Research Ethics Committees of Vice-Chancellor in Research Affairs - Tabriz University of Medical Sciences on 2023-01-30.

Funding

This project was funded by Tabriz University of Medical Sciences (grant No: 71399) under the ethical code of IR.TBZMED.VCR.REC.1401.392, and Bioscience and stem cell Technologies development council (Grant No: 11/119446).

Supplementary files

Supplementary file 1 contains Tables S1-S2 and Figs. S1-S2.

References

- Mehmood S, Faheem M, Ismail H, Farhat SM, Ali M, Younis S, et al. 'Breast cancer resistance likelihood and personalized treatment through integrated multiomics'. Front Mol Biosci 2022; 9: 783494. doi: 10.3389/fmolb.2022.783494.
- Wojtyla C, Bertuccio P, Ciebiera M, La Vecchia C. Breast cancer mortality in the Americas and Australasia over the period 1980-2017 with predictions for 2025. Biology (Basel) 2021; 10: 814. doi: 10.3390/biology10080814.
- Sopik V, Sun P, Narod SA. Impact of microinvasion on breast cancer mortality in women with ductal carcinoma in situ. Breast Cancer Res Treat 2018; 167: 787-95. doi: 10.1007/s10549-017-
- Monticciolo DL, Newell MS, Moy L, Niell B, Monsees B, Sickles EA. Breast cancer screening in women at higher-than-average risk: recommendations from the ACR. J Am Coll Radiol 2018; 15: 408-14. doi: 10.1016/j.jacr.2017.11.034.
- Song K, Farzaneh M. Signaling pathways governing breast cancer stem cells behavior. Stem Cell Res Ther 2021; 12: 245. doi: 10.1186/ s13287-021-02321-w.
- Shiozawa Y, Nie B, Pienta KJ, Morgan TM, Taichman RS. Cancer stem cells and their role in metastasis. Pharmacol Ther 2013; 138: 285-93. doi: 10.1016/j.pharmthera.2013.01.014.
- Yang L, Shi P, Zhao G, Xu J, Peng W, Zhang J, et al. Targeting cancer stem cell pathways for cancer therapy. Signal Transduct Target Ther 2020; 5: 8. doi: 10.1038/s41392-020-0110-5.
- Sousa B, Ribeiro AS, Paredes J. Heterogeneity and plasticity of breast cancer stem cells. Adv Exp Med Biol 2019; 1139: 83-103. doi: $10.1007/978 - 3 - 030 - 14366 - 4_5.$
- Yang F, He Q, Dai X, Zhang X, Song D. The potential role of nanomedicine in the treatment of breast cancer to overcome the obstacles of current therapies. Front Pharmacol 2023; 14: 1143102. doi: 10.3389/fphar.2023.1143102.
- 10. Marzoog BA. Autophagy in cancer cell transformation: a potential novel therapeutic strategy. Curr Cancer Drug Targets 2022; 22: 749-56. doi: 10.2174/1568009622666220428102741.
- Tabata K, Saeki M, Yoshimori T, Hamasaki M. How cells recognize and remove the perforated lysosome. Autophagy 2023; 19: 1869-71. doi: 10.1080/15548627.2022.2138686.
- 12. Zhen Y, Stenmark H. Autophagosome biogenesis. Cells 2023; 12: 668. doi: 10.3390/cells12040668.
- 13. Mokhtari B, Badalzadeh R. Protective and deleterious effects of autophagy in the setting of myocardial ischemia/reperfusion injury: an overview. Mol Biol Rep 2022; 49: 11081-99. doi: 10.1007/ s11033-022-07837-9.
- Mizushima N, Komatsu M. Autophagy: renovation of cells and tissues. Cell 2011; 147: 728-41. doi: 10.1016/j.cell.2011.10.026.
- 15. Janji B, Berchem G, Chouaib S. Targeting autophagy in the tumor microenvironment: new challenges and opportunities for regulating tumor immunity. Front Immunol 2018; 9: 887. doi: 10.3389/fimmu.2018.00887.
- 16. Pattabiraman DR, Weinberg RA. Tackling the cancer stem cells what challenges do they pose? Nat Rev Drug Discov 2014; 13: 497-512. doi: 10.1038/nrd4253.
- Bulgin D. Therapeutic angiogenesis in ischemic tissues by growth

- factors and bone marrow mononuclear cells administration: biological foundation and clinical prospects. Curr Stem Cell Res Ther 2015; 10: 509-22. doi: 10.2174/1574888x10666150519094132.
- Abbasi-Malati Z, Azizi SG, Zamen Milani S, Aliyari Serej Z, Mardi N, Amiri Z, et al. Tumorigenic and tumoricidal properties of exosomes in cancers; a forward look. Cell Commun Signal 2024; 22: 130. doi: 10.1186/s12964-024-01510-3.
- Verhoeven J, Baelen J, Agrawal M, Agostinis P. Endothelial cell autophagy in homeostasis and cancer. FEBS Lett 2021; 595: 1497-511. doi: 10.1002/1873-3468.14087.
- 20. Szwedowicz U, Łapińska Z, Gajewska-Naryniecka A, Choromańska A. Exosomes and other extracellular vesicles with high therapeutic potential: their applications in oncology, neurology, and dermatology. Molecules 2022; 27: 1303. doi: 10.3390/molecules27041303.
- 21. Khanicheragh P, Abbasi-Malati Z, Saghebasl S, Hassanpour P, Zamen Milani S, Rahbarghazi R, et al. Exosomes and breast cancer angiogenesis; highlights in intercellular communication. Cancer Cell Int 2024; 24: 402. doi: 10.1186/s12935-024-03606-9.
- 22. Fathi-Karkan S, Heidarzadeh M, Taghavi Narmi M, Mardi N, Amini H, Saghati S, et al. Exosome-loaded microneedle patches: promising factor delivery route. Int J Biol Macromol 2023; 243: 125232. doi: 10.1016/j.ijbiomac.2023.125232.
- 23. Théry C, Amigorena S, Raposo G, Clayton A. Isolation and characterization of exosomes from cell culture supernatants and biological fluids. Curr Protoc Cell Biol 2006; 30: 3-22. doi: 10.1002/0471143030.cb0322s30.
- Raposo G, Stoorvogel W. Extracellular vesicles: exosomes, microvesicles, and friends. J Cell Biol 2013; 200: 373-83. doi: 10.1083/jcb.201211138.
- Sokolova V, Ludwig AK, Hornung S, Rotan O, Horn PA, Epple M, et al. Characterisation of exosomes derived from human cells by nanoparticle tracking analysis and scanning electron microscopy. Colloids Surf B Biointerfaces 2011; 87: 146-50. doi: 10.1016/j. colsurfb.2011.05.013.
- Aydinlik S, Erkisa M, Cevatemre B, Sarimahmut M, Dere E, Ari F, et al. Enhanced cytotoxic activity of doxorubicin through the inhibition of autophagy in triple negative breast cancer cell line. Biochim Biophys Acta Gen Subj 2017; 1861: 49-57. doi: 10.1016/j. bbagen.2016.11.013.
- Tian T, Wang Y, Wang H, Zhu Z, Xiao Z. Visualizing of the cellular uptake and intracellular trafficking of exosomes by livecell microscopy. J Cell Biochem 2010; 111: 488-96. doi: 10.1002/ icb.22733.
- Kim MS, Haney MJ, Zhao Y, Mahajan V, Deygen I, Klyachko NL, et al. Development of exosome-encapsulated paclitaxel to overcome MDR in cancer cells. Nanomedicine 2016; 12: 655-64. doi: 10.1016/j.nano.2015.10.012.
- Zhang Y, Li M, Wang Y, Han F, Shen K, Luo L, et al. Exosome/ metformin-loaded self-healing conductive hydrogel rescues microvascular dysfunction and promotes chronic diabetic wound healing by inhibiting mitochondrial fission. Bioact Mater 2023; 26: 323-36. doi: 10.1016/j.bioactmat.2023.01.020.
- Mizushima N, Yoshimori T. How to interpret LC3 immunoblotting. Autophagy 2007; 3: 542-5. doi: 10.4161/auto.4600.
- 31. Klionsky DJ, Abdel-Aziz AK, Abdelfatah S, Abdellatif M, Abdoli A, Abel S, et al. Guidelines for the use and interpretation of assays for monitoring autophagy (4th edition)1. Autophagy 2021; 17: 1-382. doi: 10.1080/15548627.2020.1797280.
- Hassani A, Biray Avcı Ç, Kerdar SN, Amini H, Amini M, Ahmadi M, et al. Interaction of alginate with nano-hydroxyapatitecollagen using strontium provides suitable osteogenic platform. J Nanobiotechnology 2022; 20: 310. doi: 10.1186/s12951-022-01511-9.
- 33. Lee KY, Mooney DJ. Alginate: properties and biomedical applications. Prog Polym Sci 2012; 37: 106-26. doi: 10.1016/j. progpolymsci.2011.06.003.
- Licheva M, Raman B, Kraft C, Reggiori F. Phosphoregulation of the autophagy machinery by kinases and phosphatases. Autophagy 2022; 18: 104-23. doi: 10.1080/15548627.2021.1909407.

- Liu K, Chen H, Li Y, Wang B, Li Q, Zhang L, et al. Autophagy flux in bladder cancer: cell death crosstalk, drug and nanotherapeutics. Cancer Lett 2024; 591: 216867. doi: 10.1016/j.canlet.2024.216867.
- Bishop E, Bradshaw TD. Autophagy modulation: a prudent approach in cancer treatment? Cancer Chemother Pharmacol 2018; 82: 913-22. doi: 10.1007/s00280-018-3669-6.
- Nagelkerke A, Sweep FC, Geurts-Moespot A, Bussink J, Span PN.
 Therapeutic targeting of autophagy in cancer. Part I: molecular pathways controlling autophagy. Semin Cancer Biol 2015; 31: 89-98. doi: 10.1016/j.semcancer.2014.05.004.
- Hu M, Ladowski JM, Xu H. The role of autophagy in vascular endothelial cell health and physiology. Cells 2024; 13: 825. doi: 10.3390/cells13100825.
- Betus C, Heckel E, Cagnone G, Agnihotri T, Cakir B, Sapieha PM, et al. Enhancing autophagy rescues pathological angiogenesis and improves vision in a model of retinal angiomatous proliferation. *Invest Ophthalmol Vis Sci* 2023; 64: 3881.
- Chandra A, Rick J, Yagnik G, Aghi MK. Autophagy as a mechanism for anti-angiogenic therapy resistance. *Semin Cancer Biol* 2020; 66: 75-88. doi: 10.1016/j.semcancer.2019.08.031.
- Kim KW, Paul P, Qiao J, Lee S, Chung DH. Enhanced autophagy blocks angiogenesis via degradation of gastrin-releasing peptide in neuroblastoma cells. *Autophagy* 2013; 9: 1579-90. doi: 10.4161/ auto.25987.
- Hassanpour M, Rezaie J, Darabi M, Hiradfar A, Rahbarghazi R, Nouri M. Autophagy modulation altered differentiation capacity of CD146+cells toward endothelial cells, pericytes, and cardiomyocytes. Stem Cell Res Ther 2020; 11: 139. doi: 10.1186/ s13287-020-01656-0.
- Lee S, Kim H, Kim BS, Chae S, Jung S, Lee JS, et al. Angiogenesison-a-chip coupled with single-cell RNA sequencing reveals spatially differential activations of autophagy along angiogenic sprouts. *Nat Commun* 2024; 15: 230. doi: 10.1038/s41467-023-44427-0.
- Zhao Y, Xing C, Deng Y, Ye C, Peng H. HIF-1α signaling: essential roles in tumorigenesis and implications in targeted therapies. Genes Dis 2024; 11: 234-51. doi: 10.1016/j.gendis.2023.02.039.
- Yu T, Rui L, Jiumei Z, Ziwei L, Ying H. Advances in the study of autophagy in breast cancer. *Breast Cancer* 2024; 31: 195-204. doi: 10.1007/s12282-023-01541-7.
- Asano M, Tanaka S, Sakaguchi M. Effects of normothermic microwave irradiation on CD44+/CD24- in breast cancer MDA-MB-231 and MCF-7 cell lines. *Biosci Biotechnol Biochem* 2020; 84: 103-10. doi: 10.1080/09168451.2019.1670044.
- 47. Zhan Q, Yi K, Cui X, Li X, Yang S, Wang Q, et al. Blood exosomes-based targeted delivery of cPLA2 siRNA and metformin to modulate glioblastoma energy metabolism for tailoring personalized therapy. Neuro Oncol 2022; 24: 1871-83. doi: 10.1093/ neuonc/noac071.
- 48. Foretz M, Guigas B, Viollet B. Metformin: update on mechanisms of action and repurposing potential. *Nat Rev Endocrinol* **2023**; 19: 460-76. doi: 10.1038/s41574-023-00833-4.
- Putyrski M, Vakhrusheva O, Bonn F, Guntur S, Vorobyov A, Brandts C, et al. Disrupting the LC3 interaction region (LIR) binding of selective autophagy receptors sensitizes AML cell lines to cytarabine. Front Cell Dev Biol 2020; 8: 208. doi: 10.3389/ fcell.2020.00208.
- Boyer-Guittaut M, Poillet L, Liang Q, Bôle-Richard E, Ouyang X, Benavides GA, et al. The role of GABARAPL1/GEC1 in autophagic flux and mitochondrial quality control in MDA-MB-436 breast cancer cells. *Autophagy* 2014; 10: 986-1003. doi: 10.4161/auto.28390.
- Lorenzo-Gómez I, Nogueira-Recalde U, Oreiro N, Pinto-Tasende J, Blanco FJ, Carames B. HSP90AA1 is a biomarker associated with defective autophagy in osteoarhritis. *Osteoarthritis Cartilage* 2020; 28: S319. doi: 10.1016/j.joca.2020.02.494.
- Liu Q, Shi X, Zhou X, Wang D, Wang L, Li C. Effect of autophagy inhibition on cell viability and cell cycle progression in MDA-MB-231 human breast cancer cells. Mol Med Rep 2014; 10:

- 625-30. doi: 10.3892/mmr.2014.2296.
- Moldasheva A, Zhakupova A, Aljofan M. Antiproliferative mechanisms of metformin in breast cancer: a systematic review of the literature. *Int J Mol Sci* 2024; 26: 247. doi: 10.3390/ iims26010247.
- 54. Lorenzo-Gómez I, Nogueira-Recalde U, García-Domínguez C, Oreiro-Villar N, Lotz M, Pinto-Tasende JA, et al. Defective chaperone-mediated autophagy is a hallmark of joint disease in patients with knee osteoarthritis. *Osteoarthritis Cartilage* **2023**; 31: 919-33. doi: 10.1016/j.joca.2023.02.076.
- Gharoonpour A, Simiyari D, Yousefzadeh A, Badragheh F, Rahmati M. Autophagy modulation in breast cancer utilizing nanomaterials and nanoparticles. Front Oncol 2023; 13: 1150492. doi: 10.3389/fonc.2023.1150492.
- Richards T, Patel H, Patel K, Schanne F. Endogenous lipid carriersbench-to-bedside roadblocks in production and drug loading of exosomes. *Pharmaceuticals (Basel)* 2023; 16: 421. doi: 10.3390/ ph16030421.
- Niklaus NJ, Tokarchuk I, Zbinden M, Schläfli AM, Maycotte P, Tschan MP. The multifaceted functions of autophagy in breast cancer development and treatment. *Cells* 2021; 10: 1447. doi: 10.3390/cells10061447.
- 58. Cao L, Li B, Zheng S, Zhang Q, Qian Y, Ren Y, et al. Reprogramming of fibroblasts into cancer-associated fibroblasts via IGF2-mediated autophagy promotes metastasis of lung cancer cells. *iScience* **2024**; 27: 111269. doi: 10.1016/j.isci.2024.111269.
- Sadeghsoltani F, Biray Avci Ç, Hassanpour P, Haiaty S, Rahmati M, Mota A, et al. Autophagy modulation effect on homotypic transfer of intracellular components via tunneling nanotubes in mesenchymal stem cells. Stem Cell Res Ther 2024; 15: 189. doi: 10.1186/s13287-024-03813-1.
- 60. Saberianpour S, Karimi A, Nemati S, Amini H, Alizadeh Sardroud H, Khaksar M, et al. Encapsulation of rat cardiomyoblasts with alginate-gelatin microspheres preserves stemness feature in vitro. Biomed Pharmacother 2019; 109: 402-7. doi: 10.1016/j. biopha.2018.10.119.
- 61. Amini H, Hashemzadeh S, Heidarzadeh M, Mamipour M, Yousefi M, Saberianpour S, et al. Cytoprotective and cytofunctional effect of polyanionic polysaccharide alginate and gelatin microspheres on rat cardiac cells. *Int J Biol Macromol* 2020; 161: 969-76. doi: 10.1016/j.ijbiomac.2020.06.018.
- 62. Cheng HW, Chen YF, Wong JM, Weng CW, Chen HY, Yu SL, et al. Cancer cells increase endothelial cell tube formation and survival by activating the PI3K/Akt signalling pathway. *J Exp Clin Cancer Res* **2017**; 36: 27. doi: 10.1186/s13046-017-0495-3.
- 63. Hashemi M, Deldar Abad Paskeh M, Orouei S, Abbasi P, Khorrami R, Dehghanpour A, et al. Towards dual function of autophagy in breast cancer: a potent regulator of tumor progression and therapy response. *Biomed Pharmacother* **2023**; 161: 114546. doi: 10.1016/j. biopha.2023.114546.
- Vitto VA, Bianchin S, Zolondick AA, Pellielo G, Rimessi A, Chianese D, et al. Molecular mechanisms of autophagy in cancer development, progression, and therapy. *Biomedicines* 2022; 10: 1596. doi: 10.3390/biomedicines10071596.
- Walweel N, Aydin O. Enhancing therapeutic efficacy in cancer treatment: integrating nanomedicine with autophagy inhibition strategies. ACS Omega 2024; 9: 27832-52. doi: 10.1021/ acsomega.4c02234.
- 66. Guan S, Wang Y, Xie F, Wang S, Xu W, Xu J, et al. Carboxymethyl chitosan and gelatin hydrogel scaffolds incorporated with conductive PEDOT nanoparticles for improved neural stem cell proliferation and neuronal differentiation. *Molecules* 2022; 27: 8326. doi: 10.3390/molecules27238326.
- 67. Del Rocío Aguilera-Marquez J, Manzanares-Guzmán A, García-Uriostegui L, Canales-Aguirre AA, Camacho-Villegas TA, Lugo-Fabres PH. Alginate-gelatin hydrogel scaffold model for hypoxia induction in glioblastoma embedded spheroids. *Gels* 2025; 11: 263. doi: 10.3390/gels11040263.